

A 28 time-points cropland area change dataset in Northeast China from 1000 to 2020

Ran Jia^{1,3}, Xiuqi Fang^{1,2}, Yundi Yang¹, Masayuki Yokozawa³, Yu Ye^{1,2}

¹Faculty of Geographical Science, Beijing Normal University, Beijing 100875, China

²Key Laboratory of Environmental Change and Natural Disaster, Ministry of Education, Beijing Normal University, Beijing 100875, China

³Faculty of Human Sciences, Waseda University, 2-579-15 Mikajima, Tokorozawa 359-1192, Japan

Correspondence to: Yu Ye (yeyuleaffish@bnu.edu.cn)

Abstract. Based on historical documents, population data, published results, remote sensing data products, statistical data and survey data, this study reconstructed the cropland area and the spatial pattern changes at 28 time points from 1000 to 2020 in Northeast China. 1000 to 1600 corresponds to historical provincial-level administrative districts, while 1700 to 2020 corresponds to modern county-level administrative districts. The main findings are as follows: (1) The cropland in Northeast China exhibited phase changes of expansion-reduction-expansion over the past millennium. (2) the cropland area in Northeast China increased from 0.55×10^4 km² in 1000 to 37.90×10^4 km² in 2020 and the average cropland fraction increased from 0.37% to 26.27%; (3) from 1000 to 1200, the cropland area exhibited an increasing trend, peaking in 1200. The scope of land reclamation was comparable to modern times, but the overall cropland fraction remained low. The cropland area significantly decreased between 1300 and 1600, with the main land reclamation area was reduced southward into Liaoning Province. From 1700 to 1850, the cropland area increased slowly, and the agricultural reclamation gradually expanded northward. After 1850, there was almost exponential growth, with the cropland area continuously expanding to the whole study area, and the growth trend persists until 2020; (4) the dataset of changes in cropland of administrative districts in Northeast China, reconstructed based on multiple data sources and improved historical cropland reconstruction methods, significantly enhances time resolution and reliability. Additionally, the dataset shows relatively better credibility assessment results, which can provide a refined data base for historical LUCC dataset reconstruction, carbon emission estimation, climate data construction, etc. The dataset can be downloaded from <https://doi.org/10.6084/m9.figshare.25450468.v2> (Jia, 2024).

1 Introduction

Anthropogenic land cover change (ALCC) is a key driver of global change, significantly impacting climate change (Arnell et al., 2017; Foley et al., 2005; Ito and Hajima, 2020; Ellis et al., 2021; Roberts, 2019), over 70% of the Earth's land surface has undergone anthropogenic alterations over the past millennium (Sebastian et al., 2014; Shukla et al., 2019; Winkler et al., 2021). Cropland constitutes one of the primary land use types, being a land category susceptible to human influence and undergoing alterations, and it significantly influences food security, soil health, biodiversity, greenhouse gas emissions, and

31 climate change (Friedlingstein et al., 2023; Godfray et al., 2010; Kalnay and Cai, 2003; Poschlod et al., 2005). Additionally,
32 in recent years, croplands cover 12~14% of the global ice-free land (Shukla et al., 2019), Research on the long-term, accurate
33 temporal and spatial changes in cropland are crucial for understanding the carbon budget resulting from human land
34 reclamation, tracking sustainable food production, and other land-based ecosystem functions (Huang et al., 2024; Potapov et
35 al., 2022; Saez-Sandino et al., 2024; Yu and Lu, 2018).

36 Presently, various global historical Land Use and Land Cover Change (LUCC) datasets, exemplified by the History
37 Database of the Global Environment (HYDE), the Sustainability and the Global Environment (SAGE), the Pongratz Julia (PJ)
38 and the Kaplan and Krumhardt 2010 (KK10) (Goldewijk et al., 2017; Kaplan et al., 2011; Pongratz et al., 2008; Ramankutty
39 et al., 2008; Ramankutty and Foley, 1999), have been extensively employed in global change research. Such as carbon emission
40 and carbon neutrality (Xu et al., 2024), climate data construction (Gortan et al., 2024), ecological footprint (Wang et al., 2024),
41 and biological population assessment (Ye et al., 2024), etc. Furthermore, with the progress of research, historical LUCC study
42 outcomes pertaining to the Northeast China have proliferated from a global scale down to the county level (Bai et al., 2007;
43 Cao et al., 2021; He et al., 2023; Hurtt et al., 2020; Jia et al., 2023; Li et al., 2016; Li et al., 2018; Wu et al., 2020; Wu et al.,
44 2022; Yang et al., 2017; Ye et al., 2009; Ye and Fang, 2012; Yu et al., 2021; Zhang et al., 2014; Zhang et al., 2022; Zeng et al.,
45 2011; Tian, 2005; Jin et al., 2015; Shi, 2015; Zhang, 1991; Zhou, 2001). However, a disparity or uncertainty persists in the
46 standardization and spatiotemporal accuracy of the aforementioned cropland data, leading to conflicts arise between datasets
47 and historical evidence of regional agricultural development. Consequently, enhancing the accuracy and credibility of
48 historical LUCC datasets remains a focal point in international LUCC research (Gaillard et al., 2018; Yang et al., 2024; Yu et
49 al., 2021). Reconstructing relatively accurate historical cropland cover at the basic-level administrative divisions based on
50 actual historical agricultural development is a primary method for improving historical LUCC datasets (Goldewijk et al., 2017;
51 Yu et al., 2021). For instance, the HYDE dataset demonstrates a boundary effect influenced by modern provincial
52 administrative divisions in Northeast China, resulting in discontinuities in the spatial distribution of cropland in regions within
53 the same historical agricultural development process. Considering the historical evolution of administrative divisions in China
54 (Zhao et al., 2024), the cropland of smallest administrative divisions that can be reconstructed at present is the county-level,
55 which suggests that it is possible to control the error of the gridded allocation to between $0.5^{\circ} \times 0.5^{\circ}$ and $1^{\circ} \times 1^{\circ}$. Therefore,
56 long-term precise cropland area change datasets with basic-level administrative divisions and standardized time-points will
57 not merely improve the accuracy and credibility of global historical LUCC datasets, but will also play a crucial role in
58 enhancing the precision of climate and environmental simulations and supporting detailed environmental effect analyses in
59 Northeast China.

60 Northeast China is one of the most important grain bases in China today. The grain output constitutes 25.18% of the
61 national total, with corn and soybean contributing 41.64% and 56.20%, respectively (National Bureau Of Statistics, 2023). A

62 study has indicated that the supply centers for China's three major grains (wheat, corn, rice) significantly moved to the
63 Northeast from 2000 to 2020, while the demand centers did not move simultaneously. This shift underscores the rapidly
64 increasing importance of the Northeast China in ensuring China's food security (Xuan et al., 2023). Furthermore, the majority
65 of China's black soil is distributed in Northeast China, which provides an important foundation for the productivity of crops.
66 A study has pointed out that compared to other global black soil regions, the Northeast black soil region's yields of eight major
67 crops (excluding rice) remained in the top three among the world's main black soil distribution countries from 2000 to 2015,
68 with Russia and Ukraine occupying the first two positions (Wang et al., 2024). Additionally, long-term precise cropland area
69 change data reflects the significance for soil and water conservation research in Northeast China, thereby ensuring food security.
70 A typical case study in the Northeast China examined the long-term effects of cultivation on soil carbon, nitrogen, and bacterial
71 community in the Northeast black soil region. The results indicated that prolonged cultivation (e.g., 152 years) led to a
72 negatively and exponentially decline in SOC and total nitrogen (Liu et al., 2024).

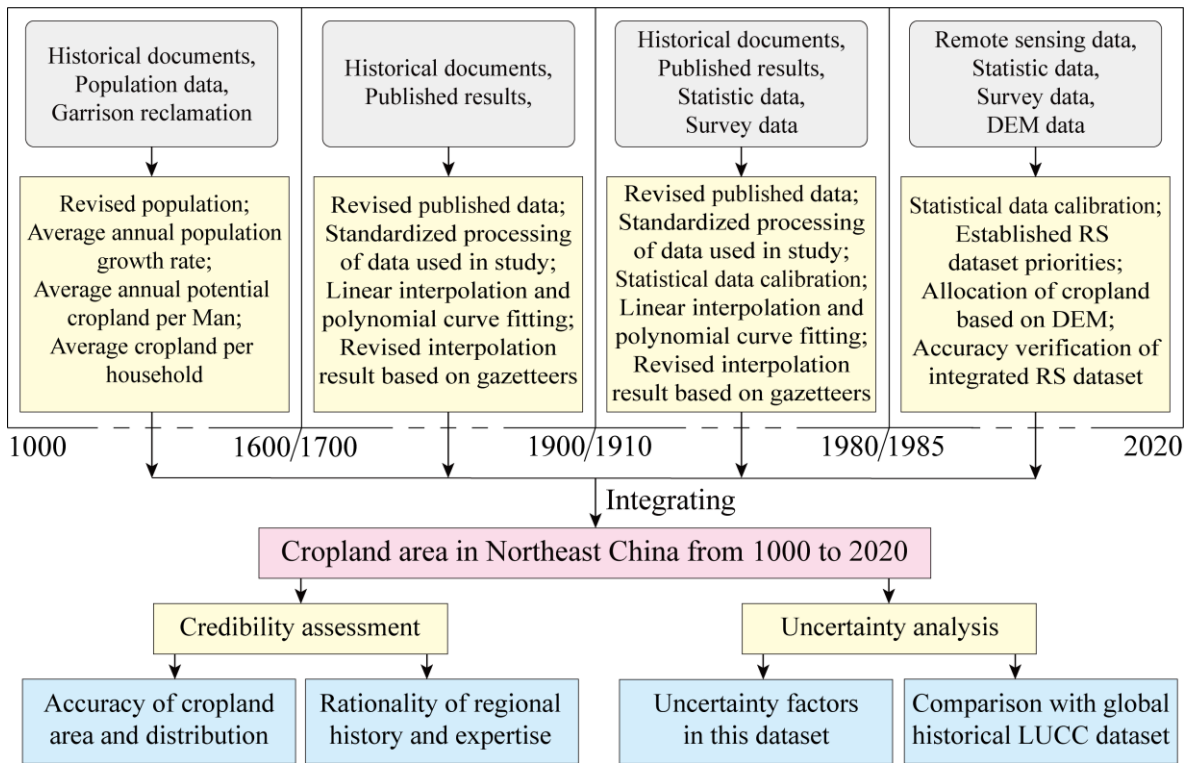
73 The dataset in this study presents a critical update and extension of the former historical cropland cover change in the
74 three provinces of Northeast China over the past 300 years (Ye et al., 2009). Throughout the prolonged agricultural
75 development, the natural vegetation landscape in the Northeast China has undergone notable transformations. In this study, we
76 used the improved historical cropland reconstruction methods to reconstruct 28 time-points cropland area by assimilating
77 multiple data sources in Northeast China from 1000 to 2020. The mainly new features of this dataset include: (1) Extended the
78 reconstruction period to 1000~2020, aligning with the standard time-points of internationally established global historical
79 LUCC datasets; (2) the reconstruction included the entire East of Inner Mongolia, which area accounts for approximately 45%
80 of the Northeast China. (3) the smallest administrative divisions for the reconstructed cropland are at the provincial-level from
81 1000 to 1600, and at the county-level from 1700 to 2020. Our main objective is to provide a long-term time series of cropland
82 area change dataset in Northeast China that is close to the historical "truth value" under a unified standard.

83 **2 Data and methods**

84 **2.1 The study area and the framework for cropland reconstruction**

85 The definition of Northeast China in this study includes Heilongjiang, Jilin and Liaoning Provinces, Hulunbuir City, Hinggan
86 League, Tongliao City, Chifeng City and Xilin Gol League of Inner Mongolia. Northeast China is located between 38°43' and
87 53°33' N and between 111°59' and 135°05' E, with a total area of approximately 1.45×10^6 km², about 15.1% of the total area
88 of China, and the main part of Northeast China has a temperate continental monsoon climate. In this study, the seven time
89 points from 1000 to 1600 are reconstructed based on the provincial-level administrative districts and derived from the
90 Historical Atlas of China (Tan, 1982a; Tan, 1982b). For the period from 1700 to 2020, twenty-one time points are reconstructed
91 based on the county-level administrative districts using the 1:1,000,000 public version of basic geographical information data

92 released by the National Geomatics Center of China (2021 edition)
 93 (<https://www.webmap.cn/commres.do?method=result100W>, last access: 10 January 2024). For the sake of convenience in
 94 research and considering the historical evolution of each region, this study consolidates the administrative districts under each
 95 prefecture-level city in the Northeast China into a single administrative unit. Additionally, Nianzishan District is merged into
 96 Longjiang County, Bayuquan District into Gaizhou City, Qingmenhe District into Fuxin County, Qinghe District into Kaiyuan
 97 City, Zhanqian District into Dashiqiao City, Zhalaينوer District into Manzhouli City, Huolinguole City into Zhalute Banner,
 98 and Aershan City into Horqin Right Wing Front Banner.



99
 100 **Figure 1: The framework for reconstructing cropland area of Northeast China from 1000 to 2020.**

101
 102 The framework of the cropland data reconstruction process in this study is illustrated in Fig. 1. It is essential to note that,
 103 unlike reconstructing historical cropland through simulation or speculation, the data foundation in this study incorporates
 104 historical literature, proxy data such as population data, revised published results, statistical data, survey data, and remote
 105 sensing data products. Historical period reconstruction primarily relies on population data from historical time points.
 106 Population data for adjacent standard time points are calculated using the average annual growth rate, and proxy indicators
 107 such as average annual cropland area per Man and average cropland area per household are employed to calculate cropland
 108 area. Additionally, after correcting published data and supplementing blank areas through standardized data processing, we
 109 used historical facts to interpolate cropland area from nearby time points to standard time points through linear interpolation.
 110 Trend extrapolation and total control are achieved through polynomial curve fitting. Finally, errors that may exist in the
 111 interpolation are corrected based on local gazetteers of China (<https://fz.wanfangdata.com.cn/>, last access: 10 January 2024).

112 The reconstruction in the modern period primarily involves analyzing the linear relationship between statistical data and survey
113 data. Survey data sequences established are used to control the cropland pixel data obtained through the regional-scale
114 constrained integration of remote sensing data.

115 **2.2 Data sources and reconstruction methods**

116 **2.2.1 Reconstruction of cropland area from 1000 to 1600**

117 This study covers seven standard time points from 1000 to 1600, spanning the Liao, Jin, Yuan, and Ming dynasties. Due to the
118 absence of direct records of cropland area during this period, cropland reconstruction primarily relies on historical documents,
119 population data, and garrison reclamation data corresponding to the provincial-level administrative districts. During the Liao
120 Dynasty period, this study based on the Dynastic History of Liao Dynasty and the History of Population in China (Wu and Ge,
121 2005a; Toqto'A, 1974) along with other published results (Ge, 2002; Han, 1999; Tan, 1982b), to reconstruct the agricultural
122 and non-agricultural populations within five provincial-level administrative districts in 1111, with an average household size
123 of 6.5 people, 2.08 of whom were Man (a male between the ages of 15 and 50 years in the Liao Dynasty). Population data for
124 the five districts in 1000 and 1100 were calculated based on a 0.5% average annual population growth rate (Wu and Ge, 2005a).

125 During the Jin Dynasty period, this study is primarily based on the Dynastic History of Jin Dynasty and the History of
126 Population in China (Wu and Ge, 2005a; Toqto'A, 1975) along with other published results (Li et al., 2018; Han, 1999; Jin and
127 Mikami, 1984; Liu, 1994a; Liu, 1994b; Tan, 1982b), to reconstruct the agricultural and non-agricultural populations within
128 five provincial-level administrative districts in 1207, with an average agricultural household size of 5.96 people, 2 of whom
129 were Man (a male between the ages of 17 and 59 years in the Jin Dynasty), while an average non-agricultural household size
130 of 10.59 people. Population data for the five districts in 1200 were calculated based on a 0.9% average annual population
131 growth rate (Toqto'A, 1975).

132 When calculating cropland area during the Liao and Jin period (1000~1200), this study primarily involves adjusting the
133 agricultural and non-agricultural population quantities to standard time points. Combining with the constructed method of the
134 average annual cropland area per Man for agricultural population and the average cropland area per household for non-
135 agricultural population during the Liao and Jin Dynasties (Jia et al., 2023), the cropland areas for provincial-level
136 administrative units in the Northeast China in the 1000, 1100, and 1200 are calculated separately (Table 1). The main algorithm
137 applied in the Liao and Jin Dynasties can be found in the supplementary materials. Furthermore, due to the lack of significant
138 technological changes in agricultural production in the Northeast China and the southward shift of the northern boundary of
139 the farming-pastoral ecotone within the study area (He et al., 2023; Han, 2012; Zhang et al., 1997), this study maintains
140 consistency with the Liao and Jin Dynasties. The average annual cropland area per Man for agricultural population is set at 14
141 *Mu* (0.93 hm^2), and the average cropland area per household for non-agricultural population is set at 2 *Mu* (0.13 hm^2) during

142 the Yuan and Ming Dynasties (1300~1600).

143 During the Yuan Dynasty, this study primarily based on the Dynastic History of Yuan Dynasty (Song, 1976) to obtain the
144 garrison reclamation area and corresponding number of soldiers in the Northeast China around 1300, and the average cropland
145 area per garrison soldier is 100.1 *Mu* (6.67 hm²). Additionally, based on the Dynastic History of Yuan Dynasty and the History
146 of Population in China (Wu and Ge, 2005a; Cao and Ge, 2005b; Song, 1976) along with other published results (Cong, 1993a;
147 Zhan, 2017; Xue, 2012; Zhou, 2021), this study reconstructs the number of ordinary households and Mongol households within
148 the three provincial-level administrative districts of the study area during the Yuan Dynasty (Tan, 1982a). Ordinary households
149 are further divided into Han households (agricultural population) and other minority ethnic households (non-agricultural
150 population) in a 7:3 ratio (Cong, 1993b), with an average agricultural household size of 5 people, 1.67 of whom were Man (a
151 male between the ages of 15 and 59 years in the Yuan Dynasty). Population data for garrison soldiers, Han households, minority
152 ethnic households, and Mongol households in the three districts around 1300 are calculated based on different average annual
153 population growth rates ranging from 0.6% to 1.8% during the Yuan Dynasty (Wu and Ge, 2005a). After obtaining the
154 population data, this study subtracts the garrison soldiers and their corresponding households from the ordinary households.
155 Subsequently, the remaining ordinary households are divided into Han households and minority ethnic households in a 7:3
156 ratio. The cropland area for agricultural population is calculated based on the average annual cropland area per Man for
157 agricultural population, while the cropland area for non-agricultural population, including Mongol households, is calculated
158 using the average cropland area per household for non-agricultural population referring the Liao and Jin Dynasties (Table 1).

159 During the Ming Dynasty, this study primarily based on the Dynastic History of Ming Dynasty (Zhang, 1974) to obtain
160 the garrison reclamation area in the Northeast China around 1400. According to historical records and verification, it is
161 determined that each garrison soldier in the Liaodong region possessed 46 *Mu* (3.07 hm²) of cropland, with the proportion of
162 garrison soldiers among soldiers being approximately 30%, and the number of dependents for each soldier being twice that of
163 soldiers (Cao and Ge, 2005b; Li, 2019; Wang, 2009; Zhang, 1974). Additionally, based on the Dynastic History of Ming
164 Dynasty and the History of Population in China (Cao and Ge, 2005b; Zhang, 1974) along with other published results (Cong,
165 1985; Kong and Feng, 1989; Li, 2019; Tan, 1982a), this study reconstructs the population of soldiers and their dependents,
166 ordinary households/aborigines, and the population of minority ethnic households and Mongols (non-agricultural population)
167 within the four provincial-level administrative districts in the 1400. Referring to historical records such as refugee migration,
168 the construction of the Great Wall, and supplementary border garrisons (Cao and Ge, 2005b; Kong and Feng, 1989; Liu et al.,
169 2016; Tan, 1982a), the historical maps for the 1500 and 1600 are divided into three provincial districts, and the population data
170 for these two time points is obtained based on the aforementioned historical documents. During this period, all regular soldiers
171 in the Dusi of Eastern Liao and one-third of their dependents would operate cropland as farmers. The average agricultural
172 household (ordinary households/aborigines/refugees/migrants) size of 6, 2.25 of whom were Man (a male between the ages of

173 16 and 60 years in the Ming Dynasty) in the Dusi of Eastern Liao. The average non-agricultural household (minority ethnic
 174 households) size of 6, 2 of whom were Man in the Dusi of Nuergan, while size of the Mongol households is 5, 1.67 of whom
 175 were Man. Population data for soldiers and their dependents, ordinary households/aborigines/refugees/migrants, minority
 176 ethnic households in the Dusi of Nuergan, and Mongol households in the western part of the study area in the three provinces
 177 are calculated for the 1500 and 1600 based on average annual population growth rates of 0.8%, 0.5%, 0.2%, and 0.15%,
 178 respectively (Cao and Ge, 2005b). After obtaining the population data, we calculated the garrison reclamation area and civilian
 179 cropland area within the Dusi of Eastern Liao and the Dusi of Beiping based on the population of soldiers and agricultural
 180 population (ordinary households/aborigines) in the 1400. The minority ethnic population in the Dusi of Nuergan and the
 181 Mongol population in the Dada are calculated as non-agricultural population referring the Liao and Jin Dynasties (Table 1).
 182 For the 1500 and 1600, we calculated the garrison reclamation area and civilian cropland area within the Dusi of Eastern Liao
 183 based on the population of soldiers and agricultural population (ordinary households/aborigines/refugees/migrants). The
 184 minority ethnic population in the Dusi of Nuergan and the Mongol population in the Dada are calculated as non-agricultural
 185 population referring the Liao and Jin Dynasties (Table 1). The main algorithm applied in the Yuan and Ming Dynasties can be
 186 found in the supplementary materials.

187
 188 **Table 1: The index of cropland area reconstruction from 1000 to 1600**

Period	Population type	Population (10 ⁴)	Proportion of household registration	Corresponding cropland area	Total cropland area (km ²)
1000, 1100	Agricultural population	371(1000); 612(1100)	Average household size: 6.5 people, 2.08 of whom were Man	Average annual cropland area per Man is 14 <i>Mu</i> (0.93 hm ²)	5513(1000); 9078(1100)
	Non-agricultural population	140(1000); 231(1100)		Average cropland area per household is 2 <i>Mu</i> (0.13 hm ²)	
1200	Agricultural population	587	Average household size: 5.96 people, 2 of whom were Man	Average annual cropland area per Man is 14 <i>Mu</i> (0.93 hm ²)	16949
	Non-agricultural population	338	Average household size: 10.59 people	Average cropland area per household is 45.3 <i>Mu</i> (3.02 hm ²)	
1300	Garrison soldiers	0.8	Each soldier represents a household	Average per garrison soldier is 100.1 <i>Mu</i> (6.67 hm ²)	4350
	Agricultural population	111	Average household size: 5 people, 1.67 of whom were Man	Average annual cropland area per Man is 14 <i>Mu</i> (0.93 hm ²)	
	Non-agricultural population (Minority ethnic household)	137		Average cropland area per household is 2 <i>Mu</i> (0.13 hm ²)	
1400	Soldiers and their dependents	70	Approximately 30% of garrison soldiers; Soldiers : dependents = 1 : 2	Average per garrison soldier is 46 <i>Mu</i> (3.07 hm ²)	2790
	Agricultural population (ordinary)	10	Average household size: 6 people, 2.25 of whom were	Average annual cropland area per Man is 14 <i>Mu</i> (0.93 hm ²)	

	households/aborigines)		Man		
	Non-agricultural population (Minority ethnic household, Mongol household)	40	Average minority ethnic household size: 6 people, 2 of whom were Man; Mongol household size: 5, 1.67 of whom were Man	Average cropland area per household is 2 <i>Mu</i> (0.13 hm ²)	
1500, 1600	Soldiers and their dependents	25(1500); 12(1600)	Approximately 30% of garrison soldiers; Soldiers : Dependents = 1 : 2	Average per garrison soldier is 46 <i>Mu</i> (3.07 hm ²); Regular soldiers and one-third of their dependents is 14 <i>Mu</i> (0.93 hm ²)	4875(1500); 5868(1600)
	Agricultural population (ordinary households/aborigines/refugees/migrants)	83(1500); 137(1600)	Average household size: 6 people, 2.25 of whom were Man	Average annual cropland area per Man is 14 <i>Mu</i> (0.93 hm ²)	
	Non-agricultural population (Minority ethnic household, Mongol household)	68(1500); 81(1600)	Same as 1400	Average cropland area per household is 2 <i>Mu</i> (0.13 hm ²)	

189

190 **2.2.2 Reconstruction of cropland area from 1700 to 1900**

191 The reconstruction of cropland in this study at five standard time-points from 1700 to 1900 is primarily based on published
192 results and historical documents. Among them, published results utilize the county-level cropland fraction data (CNEC)
193 reconstructed by Ye (Ye et al., 2009) for the three provinces in Northeast China in 1683, 1735, 1780, and 1908. Additionally,
194 data on cropland fraction for 15 counties and districts, including Chifeng City, Balinzuo Banner, Balinyou Banner, Linxi
195 County, Wengniute Banner, Kalaqin Banner, Ningcheng County, Aohan Banner, Kulun Banner, Naiman Banner, Taipusi
196 Banner, Xianghuang Banner, Zhengxiangbai Banner, Zhenglan Banner, and Duolun County, reconstructed by Tian (Tian, 2005),
197 are available for the years 1724, 1782, 1868, and 1911. Detailed description of the data and methods for these published results
198 can be found in the supplementary materials.

199 Before utilizing the published results, this study examined and corrected issues present in the data, unifying it onto the
200 base map used in this study. (1) Correction of published results: CNEC data (Ye et al., 2009) was adjusted based on the
201 historical evolution of administrative boundaries to modern county-level administrative units. In 1908, cropland areas were
202 missing for Qian Gorlos Mongolian Autonomous County, Jiaohe City, Yanji City, Wangqing County, Huichun City, Helong
203 City, and Huinan County in Jilin Province. Wu (Wu, 2021) interpolated these missing values using the principles of
204 geographical proximity and similarity in the regional agricultural development stage. By following the above method, we
205 interpolated data for problematic counties in Jilin Province from CNEC data using settlement names evolution data for the
206 past 300 years (Zeng et al., 2011). It is worth noting that for certain time points, due to the absence of cropland in neighboring
207 counties, this study adopted the approach of multiplying the cropland area owned by unit settlements within Jilin Province at

208 that time by the number of settlements in the respective county to obtain the cropland area (Table S1). Furthermore,
209 discrepancies were identified in used CNEC data for some counties in Heilongjiang and Liaoning provinces compared to
210 published data. This study corrected these inconsistencies after verifying historical documents (Table S1).

211 (2) Unified administration boundaries: The CNEC data (Ye et al., 2009) in 1683, 1735, and 1780 corresponds to historical
212 Qing Dynasty administrative districts, and the administrative districts used in 1908, 1914, 1931, 1940, 1950, and 1980 also
213 differed from that of this study. The approach taken in this study involves unifying the cropland fraction within each county or
214 district. The modern county-level administrative vector map used in this study is overlaid with Ye's county-level cropland
215 fraction map. Then we calculated the area of overlap between each county or district in this study and Ye's corresponding
216 county or district and then calculates the cropland area based on the proportional statistics. Similarly, for the Tian's data (Tian,
217 2005) used in this study for cropland fraction in 1724, 1782, 1868, 1911, and 1933, the same method is applied to unify them
218 onto the modern map used in this study.

219 (3) Linear interpolation and polynomial curve fitting to obtain the cropland area: Previous studies have used the linear
220 interpolation and polynomial curve fitting to reconstruct cropland areas (He et al., 2017; Jin et al., 2015; Ramankutty and Foley,
221 1999; Wei et al., 2016; Wei et al., 2021; Ye et al., 2015; Yu, 2019; Fang et al., 2021), and the interpolated data did not reduce
222 the credibility of their datasets. In addition, previous studies have shown that in the process of reclamation in the Northeast
223 China over the past 300 years, 1860 was a dividing point between slow growth and rapid growth, mainly due to the
224 implementation of the immigration and reclamation policy by the Qing government (Fang et al., 2020; Ye et al., 2009; Fang et
225 al., 2005; Kong and Feng, 1989). Therefore, this study selected the CNEC data (Ye et al., 2009) in 1683, 1735, 1780, 1908 and
226 1914 for linear interpolation and polynomial curve fitting of cropland area data for each county or district in the three provinces
227 of Northeast China, obtaining data for 1700, 1750, 1800, 1850 and 1900. In addition, this study selected the data from Tian
228 (Tian, 2005) in 1724, 1782, 1868, and 1911; the CNEC data (Ye et al., 2009) in 1735; the data from Ye (Ye and Fang, 2012)
229 in 1916 for linear interpolation and polynomial curve fitting to obtain cropland area data for 1700, 1750, 1800, 1850, and 1900
230 in the Eastern of Inner Mongolia. The problems that may be encountered during the operation and the corresponding solutions
231 are as follows:

232 ①Linear interpolation and determination of zero values. The time points involved in this issue include 1700 and 1750 for
233 the three provinces of Northeast China; 1750, 1800, and 1850 for East of Inner Mongolia. For instance, in Northeast China,
234 the cropland area in each county in 1700 is interpolated based on records from 1683 and 1735. At 1700, there are no negative
235 values, but there may be zero values. Specifically, the cropland value in 1683 is 0, while there is definite value in 1735. Our
236 solution involves consulted contemporary county gazetteers to verify the history of land reclamation in 1700. If so, a
237 polynomial curve fitting trend extrapolation was applied to obtain the proportional relationship at the provincial level for
238 adjacent points on the extrapolated trend. Then this proportion was multiplied by the cropland area of the county at the adjacent

239 time-point to obtain the cropland area at that time-point. If the land was not reclaimed, the value at that time point was
240 considered as zero. Similarly, other counties involved in interpolation adopt the same solution when encountering this situation.

241 ②Polynomial curve fitting and correction of negative values. Besides the previously mentioned linear interpolation,
242 polynomial curve fitting based on the least squares method may encounter problems with data points resulting in negative
243 values. First of all, the main reason for this issue is our historical determination that 1860 was a dividing point between slow
244 and rapid growth. Therefore, we use 1860 as a breakpoint and separate interpolated the data for Ye (Ye et al., 2009, Ye and
245 Fang, 2012) and Tian (Tian, 2005) before and after this period. Second, for time points that cannot be directly obtained through
246 linear interpolation, cropland need to be calculated by polynomial fitting backwards (1800 and 1850 in the three provinces of
247 Northeast China; 1900 in East of Inner Mongolia). For instance, in Northeast China, cropland area in each county in 1800 and
248 1850 are derived from data in 1683, 1735, and 1780 using polynomial curve fitting method. Some counties may show a decline
249 in cropland, potentially resulting in negative values in the extrapolation results. Our solution involves using the proportion of
250 provincial administrative level to multiply by the cropland area in 1780 for correction in the counties' cropland area in 1800
251 and 1850. Third, for time points that cannot be directly obtained through linear interpolation, cropland need to be calculated
252 by polynomial fitting forwards (1900 in the three provinces of Northeast China; 1700, 1910 in East of Inner Mongolia). For
253 instance, in Northeast China, cropland area in each county in 1900 is derived from data in 1908 and 1914 using polynomial
254 curve fitting method. Due to rapid growth of cropland in some counties from 1908 to 1914, the extrapolation for 1900 may
255 result in negative values. Our solution involves using the proportion of provincial administrative level to multiply by the
256 cropland area in 1908 for correction in the counties' cropland area in 1900.

257 It should be noted that, considering the historical development process of Northeast China during the Qing Dynasty, war
258 factors, and the encouraging land reclamation policies implemented by the Qing government after 1860, we determined that
259 the cropland area in each county of Northeast China in 1900 would not significantly exceed that of 1908. During this period,
260 in Northeast China, the total cropland area was gradually increasing and was not significantly affected by events such as the
261 Second World War, which led to a notable decrease in cropland area in 1950 compared to 1930 and 1940. Therefore, when the
262 extrapolated value for a county in 1900 exceeds that of 1908, the proportion of provincial administrative level is used to
263 multiply by the cropland area in 1908 for correction in the county's cropland area in 1900.

264 ③The determination of initial cultivation occurred between 1780 and 1908. Few counties in Northeast China where
265 cropland was zero in 1683, 1735, and 1780, but had cropland in 1908. Our solution involves consulted contemporary county
266 gazetteers to verify the history of land reclamation between 1800 and 1900. If local gazetteers indicate the initial cultivation
267 occurred before 1860, this study applies the same method as described in “①Linear interpolation and determination of zero
268 values”. If the initial cultivation began after 1860, this study applies the same method as described in “②Polynomial curve
269 fitting and correction of negative values”. All the counties where this situation occurs can be found in Table S2.

270 2.2.3 Reconstruction of cropland area from 1910 to 1980

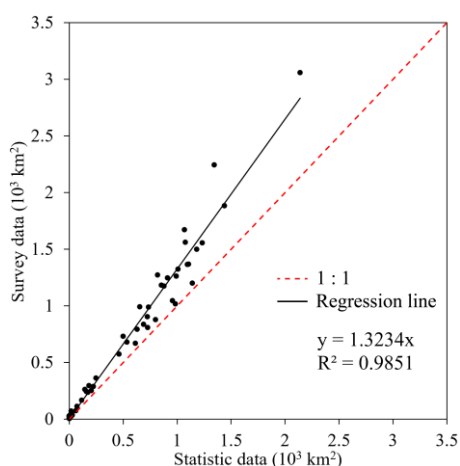
271 The reconstruction of cropland at eight standard time points from 1910 to 1980 in this study is mainly based on published
272 results, historical documents, statistical data, and survey data. Among these, the published results include the cropland fraction
273 for the three provinces in Northeast China in 1908, 1914, 1931, 1940, 1950, and 1980 (CNEC) (Ye et al., 2009). As well as the
274 cropland fraction for the farming-pastoral ecotone area reconstructed by Ye in 1916 and 1940 (Ye and Fang, 2012). Additionally,
275 Tian's reconstruction provides cropland fraction for 15 counties in the Eastern of Inner Mongolia in 1911 and 1933 (Tian,
276 2005). Historical documents include the Summary of county governance in Northeast China (Xiong, 1933) to supplement
277 cropland area data for the Eastern of Inner Mongolia in 1931. Statistical data include Agricultural and Animal Husbandry
278 Production Statistics (Inner Mongolia Provincial Bureau Of Statistics, 1983) to obtain county-level cropland area for the
279 Eastern of Inner Mongolia in 1950, 1960, 1970, and 1980. Survey data include Manchuria Economic Statistics Charts (Office
280 Of The Governor-General Of Kwantung, 1918) to obtain prefecture-level cropland area data for the Eastern of Inner Mongolia
281 in 1917 as a reference. The North Manchuria and East Support Railway (East Branch Railway Administration Of Russia and
282 South Manchuria Railways Co., 1923) is used as survey data to supplemented for various counties in the Eastern of Inner
283 Mongolia in 1911 and 1914, which was not covered by existing data from Ye and Tian. Additionally, a digital version of the
284 Manchuria Political Map from this document was used to obtain county-level district maps for Northeast China in the 1920s.
285 Detailed description of the data and methods for these published results can be found in the supplementary materials.

286 Before using the published data from this period, this study also assessed and corrected the issues present in the data.
287 Additionally, when supplementing the data using historical documents, statistical data and survey data, this study referred to
288 the data processing methods of the aforementioned published studies. (1) Correction of published results: This study has
289 provided specific explanations for the correction of CNEC data for this period in previous sections, as detailed in Table S1.

290 (2) Standardization of Data: This study adopted the processing method used by Ye (Ye et al., 2006) for the Summary of
291 county governance in Northeast China (Xiong, 1933). It converted the Qing Dynasty's *Mu* unit to the standard unit of
292 measurement, square kilometers (km²), and made a 10% correction to align this data with the survey data. For the Manchuria
293 Economic Statistics Charts and the North Manchuria and East Support Railway (Office Of The Governor-General Of
294 Kwantung, 1918), this study followed Ye's (Ye et al., 2006) analysis method for similar survey data, treating it as the actual
295 cropland area. Regarding the standardization of administrative boundaries, this study utilized the digitized Manchurian
296 Political Map and employed the method aforementioned to map it onto the modern administrative boundary map used in this
297 study. The standardization of measurement units followed the conversion from the measurement units used in the Japanese
298 survey data to the universal unit of measurement, square kilometers (km²), as per Weights and Measures in Northeast China
299 (South Manchuria Railways Co., 1927).

300 (3) Correlation analysis between statistical data and survey data: In this study, we referred the method used by Ye (Ye et

301 al., 2009) in analyzing statistic data for the simultaneous period in the three provinces in Northeast China to process the county-
 302 level cropland area statistical data for the 1950, 1960, 1970, and 1980 in the Eastern of Inner Mongolia (Inner Mongolia
 303 Provincial Bureau Of Statistics, 1983). It is found a stronger correlation between the statistical data and land survey data in
 304 1985 (National Bureau Of Statistics, 1989; Committee Of Integrative Survey Of Natural Resources and Committee Of National
 305 Planning Of Chinese Academy Of Sciences, 1990), with a linear regression equation of $y=1.3234x$ and $R^2=0.9851$ (Fig. 2).
 306 That means the land survey data in the Eastern of Inner Mongolia is approximately 32.34% higher than the corresponding
 307 statistical data, then corrected cropland area data by 32.34% for each county in the Eastern of Inner Mongolia for the 1950,
 308 1960, 1970, and 1980.



310 **Figure 2: Correlation between the statistical cropland data and survey cropland data of the counties in the Eastern of Inner Mongolia**
 311 **in 1980's.**

313

314 (4) Linear interpolation and polynomial curve fitting to obtain the cropland area: This study selected CNEC (Ye et al.,
 315 2009) data in 1908 and 1914 for linear interpolation and polynomial curve fitting of cropland area data for each county or
 316 district in the three provinces of Northeast China, obtaining data for 1910 and 1920. Additionally, this study selected the data
 317 from Tian (Tian, 2005) in 1911 and the data from Ye (Ye and Fang, 2012) in 1916 and 1940, and the corrected data in 1931
 318 from Summary of county governance in Northeast China (Xiong, 1933) for linear interpolation and polynomial curve fitting
 319 of cropland area data for each county or district in the Eastern of Inner Mongolia, obtaining data for 1910 and 1920. Since the
 320 following operations are the same as 1700~1900, and the problems that may be encountered during the operation and the
 321 corresponding solutions have been detailed above, it will not be repeated here.

322 It should be noted that this study considers the corrected data in 1931 in various counties of the Northeast China as data
 323 for 1930. In addition, the cropland area data for the year 1940 mainly based on the corrected published results. For the missing
 324 data in single-digit counties of the Eastern of Inner Mongolia, this study uses data recorded in local gazetteers to fill in the
 325 gaps.

326 **2.2.4 Reconstruction of cropland area from 1985 to 2020**

327 The reconstruction of cropland in this study from 1985 to 2020 at eight standard time points is primarily based on remote
 328 sensing data products, statistical data, survey data, and DEM data. Among these, eight sets of remote sensing data products
 329 were used (Table 2): AGLC (Xu et al., 2021), CLDC (Yang and Huang, 2021), ESA_WorldCover (Zanaga, 2021),
 330 Esri_LandCover (Karra et al., 2021), FROM_GLC (Gong et al., 2013), GFSAD30 (Thenkabail et al., 2021), GLC_FCS30
 331 (Zhang et al., 2023), GlobeLand30 (Chen et al., 2015). It is worth mentioning that we conducted research on ESA_WorldCover
 332 and Esri_LandCover after resampling them to a resolution of 30 meters. Survey data includes the year 1985 county-level first
 333 general land investigation (Committee Of Integrative Survey Of Natural Resources and Committee Of National Planning Of
 334 Chinese Academy Of Sciences, 1989), provincial-level data from the first national land survey (Li, 2000), prefecture-level data
 335 from the second national land survey, and county-level data from the third national land survey (<https://gtdc.mnr.gov.cn/Share#/>,
 336 last access: 10 January 2024).

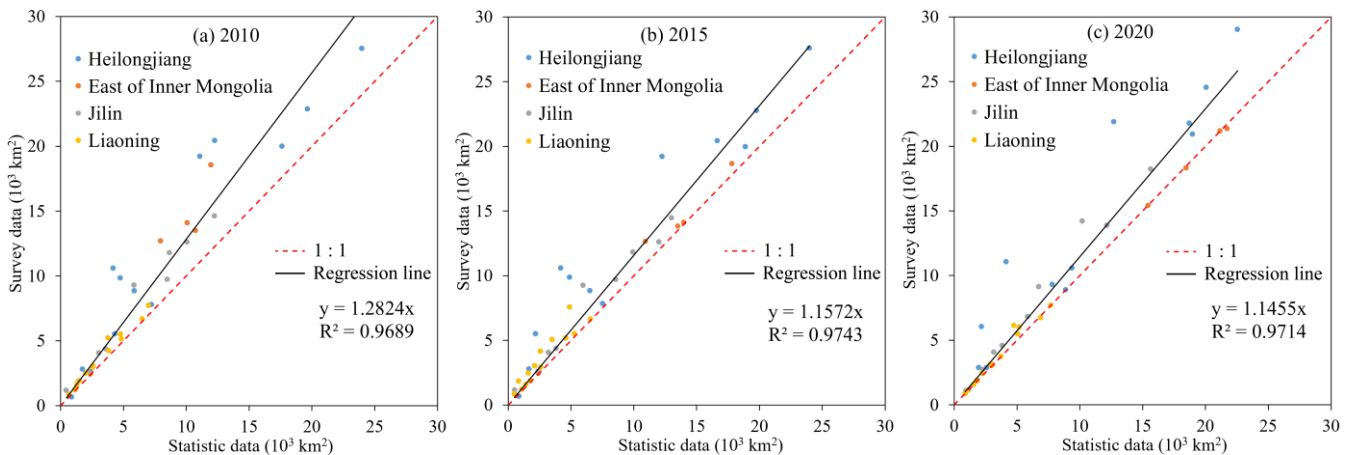
337
 338 **Table 2: Characteristics of the eight RS products**

Product	Satellite Sensor	Type	Resolution	Year	Cropland Classes	URL	Reference
AGLC	Landsat 5 TM Landsat 7 ETM+ Landsat 8 OLI	Boolean	30m	2000, 2005, 2010, 2015	10.Cropland	https://code.earthengine.google.com/?asset=users/xxc/GLC_2000_2015 [2024/01/10]	(Xu et al., 2021)
CLDC	Landsat 8 OLI TM ETM+	Boolean	30m	1985, 1990, 1995, 2000, 2005, 2010, 2015, 2019	1.Cropland	https://doi.org/10.5281/zenodo.4417810 [2024/01/10]	(Yang and Huang, 2021)
ESA_WorldCover	Sentinel-1 Sentinel-2	Boolean	10m	2020	40.Cropland	https://viewer.esa-worldcover.org/worldcover/ [2024/01/10]	(Zanaga, 2021)
Esri_LandCover	Sentinel-2	Boolean	10m	2020	5.Crops	https://livingatlas.arcgis.com/landcover/ [2024/01/10]	(Karra et al., 2021)
FROM_GLC	Landsat TM, ETM+, OLI	Boolean	30m	2010, 2015	10.Cropland	https://data-starcloud.pcl.ac.cn/zh [2024/01/10]	(Gong et al., 2013)
GFSAD30	Landsat ETM+ OLI	Boolean	30m	2015	2.Cropland	https://lpdaac.usgs.gov/products/gfsad30aunzcnmocev001/ [2024/01/10]	(Thenkabail, 2021)
GLC_FCS30D	Landsat OLI	Boolean	30m	1985, 1990,	10.Rainfed cropland	https://zenodo.org/records/8239305 [2024/01/10]	(Zhang et al., 2023)

				1995, 2000, 2005, 2010, 2015, 2020	11.Herbaceous cover 12.Tree or shrub cover (Orchard) 20.Irrigated cropland		
GlobeLand3 0	Landsat TM/ETM+, HJ- 1	Boolean	30m	2000, 2010, 2020	10.Cropland	http://www.webmap.cn/map/DataAction.do?method=globeLandCover [2024/01/10]	(Chen et al., 2015)

339

340 In this study, based on remote sensing data products, statistical data, survey data, and DEM data, we have developed a
341 constrained integration method that combines multisource cropland cover products with survey data. (1) Correlation analysis
342 between statistical data and survey data: This study obtained cropland survey data at the county-level in 1985, at the provincial-
343 level in 1996, at the prefecture-level in 2010 and 2015, and at the county-level in 2020. It should be noted that the 2015
344 cropland survey data was obtained through the annual land change survey based on the second NLS, which is relatively less
345 accurate than the cropland areas from the standard time-points data after the nationwide surveys (e.g., 2010 and 2020).
346 According to the Ministry of Natural Resources of the PR China, the annual land change survey is based on the results of the
347 nationwide survey and the previous year's land change survey, examining the current status and changes in the land use class,
348 location, area, and distribution of various urban and rural lands across the country at the end of each year. For the missing
349 years 1990, 2000, and 2005, this study referred to the correlation analysis between modern survey data and statistical data (Ye
350 et al., 2009; Cropland Research Group, 1992). This study selected survey data and statistical data from 2010, 2015, and 2020
351 within the study area, respectively, and established linear regression equation between them. The results showed that the linear
352 regression equation was $y=1.2824x$ in 2010, and $R^2=0.9689$; $y=1.1572x$ in 2015, and $R^2=0.9743$; $y=1.1455x$ in 2020, and
353 $R^2=0.9714$ (Fig. 3, Table S4). This indicates a high correlation between the two types of data at the three time points, and the
354 survey data is approximately 14.6% to 28.2% higher than the statistical data at the same period, with an average of about 20%,
355 then corrected cropland area data by 20% for each county in the study area for the 1990, 2000 and 2005.



356

357 **Figure 3: Correlation between the statistical cropland data and survey cropland data at the prefecture-level in the Northeast China**

358 in 2010, 2015 and 2020.

359

360 (2) Establishing Dataset Priorities: After obtaining the modern land survey data levels for each province in the study area
361 at five-year intervals from 1985 to 2020, the difference between the cropland area in dataset i and the survey data on cropland
362 area, denoted as $D_{i,j}$, was calculated to evaluate the accuracy of the dataset, as shown in Equation (1):

$$363 \quad D_{i,j} = abs\left(\frac{A_{s,j} - a_{i,j}}{A_{s,j}}\right), \quad (1)$$

364 where $A_{s,j}$ represents the survey data on cropland area in Northeast China for year j , and $a_{i,j}$ represents the cropland area in the
365 i -th subset of the land cover product for year j . The value of $D_{i,j}$ is lower when the consistency with survey data is higher,
366 indicating a higher priority for the input dataset. It should be noted that in this study, based on the priority and overlap of
367 remote sensing data products used at different time points, pixels in the study area are ranked. Pixels belonging to high-priority
368 products with high overlap will be prioritized as cropland.

369 (3) Allocation of cropland pixels based on DEM data: The survey data includes detailed slope classification, and the
370 slopes were categorized into five classes: $<2^\circ$, $2\sim6^\circ$, $6\sim15^\circ$, $15\sim25^\circ$, and $>25^\circ$, and the corresponding cropland areas for each
371 slope class were recorded. In this study, we selected NASA and METI's DEM data jointly released in 2019: ASTER Global
372 Digital Elevation Model V003 30m. The ASTER Global Digital Elevation Model V003 can be downloaded from the NASA
373 EARTHDATA website (<https://www.earthdata.nasa.gov/>, last access: 10 January 2024). Pixels prioritized as cropland were
374 allocated to the cropland area corresponding to each slope level in the survey data. The distribution results were controlled by
375 provincial-level cropland area survey data at different time points, resulting in the integration of cropland data at 30m resolution
376 for the Northeast China at 8 time points from 1985 to 2020.

377 (4) Accuracy assessment and validation of RS products integration results: This study utilizes the confusion matrix was
378 used to assess the accuracy of cropland products. The Producer Accuracy (P.A.) and User Accuracy (U.A.) for each product in
379 2020 are calculated as two indicators to evaluate the reliability of the spatial distribution of the cropland dataset. The calculation
380 methods are as follows:

$$381 \quad P.A. = \frac{X}{N_i} \times 100\% , \quad (2)$$

$$382 \quad U.A. = \frac{X}{N_j} \times 100\% , \quad (3)$$

383 where X represents the number of correctly classified samples, N_i represents the total number of verification samples, and N_j
384 represents the total number of samples in the classified result.

385 This study used three types of verification points for the verification of the integration result in year 2020 (Fig. S1): (1)
386 346 cropland sample points located in the study area from FROM-GLC. (2) 1052 sample points obtained through field

387 investigations conducted by the authors in April 2023 within the study area. (3) A total of 1200 random sample points were
388 generated within the study area. Using high-resolution imagery from Google Earth captured in 2020, the sample points were
389 visually interpreted and validated indoors through image comparison. The results show that the producer accuracy for cropland
390 pixels is 94.85%, and the user accuracy is 96.49% in year 2020. For non-cropland pixels, the producer accuracy is 91.12%,
391 and the user accuracy is 87.32%. The overall accuracy is relatively high.

392

393 **3 Results**

394 The cropland in Northeast China exhibited phase changes of expansion-reduction-expansion over the past millennium. The
395 cropland area in Northeast China increased from $0.55 \times 10^4 \text{ km}^2$ in 1000 to $37.90 \times 10^4 \text{ km}^2$ in 2020 and the average cropland
396 fraction increased from 0.37% to 26.27% (Fig. 4). Our results clearly show on the map the process of agricultural reclamation
397 in Northeast China and the expansion of cropland in the Songnen and Sanjiang Plains (Fig. 5).

398 **3.1 Changes in the historical cropland area in Northeast China over the past millennium**

399 The changes in cropland area in the Northeast China over the past millennium are illustrated in Figure 4. Overall, the proportion
400 of cropland area in the study area from 1000 to 1600 ranged from 0.74% to 4.5% of the total in 2020. During this period, from
401 1000 to 1200, the cropland area showed a growing trend, with an average annual growth rate of 0.56%. In 1200, it peaked at
402 $1.69 \times 10^4 \text{ km}^2$, with an overall cropland fraction of 1.17%, although the cropland fraction across the region was relatively low.
403 From 1300 to 1600, the cropland area significantly decreased. In 1400, it reached the lowest point in the past millennium, at
404 $0.28 \times 10^4 \text{ km}^2$, with an overall cropland fraction of only 0.19%. The average annual growth rate from 1400 to 1600 was 0.37%.
405 From 1600 to 1850, the cropland area grew slowly, with an average annual growth rate of 0.81%. During this period, the
406 proportion of cropland area in the study area increased from 1.55% to 11.52% of the total in 2020. After 1850, the cropland
407 area exhibited almost exponential growth. The agricultural area continued to expand northward, and this growth trend persisted
408 until 2020, with an average annual growth rate of 1.28%.

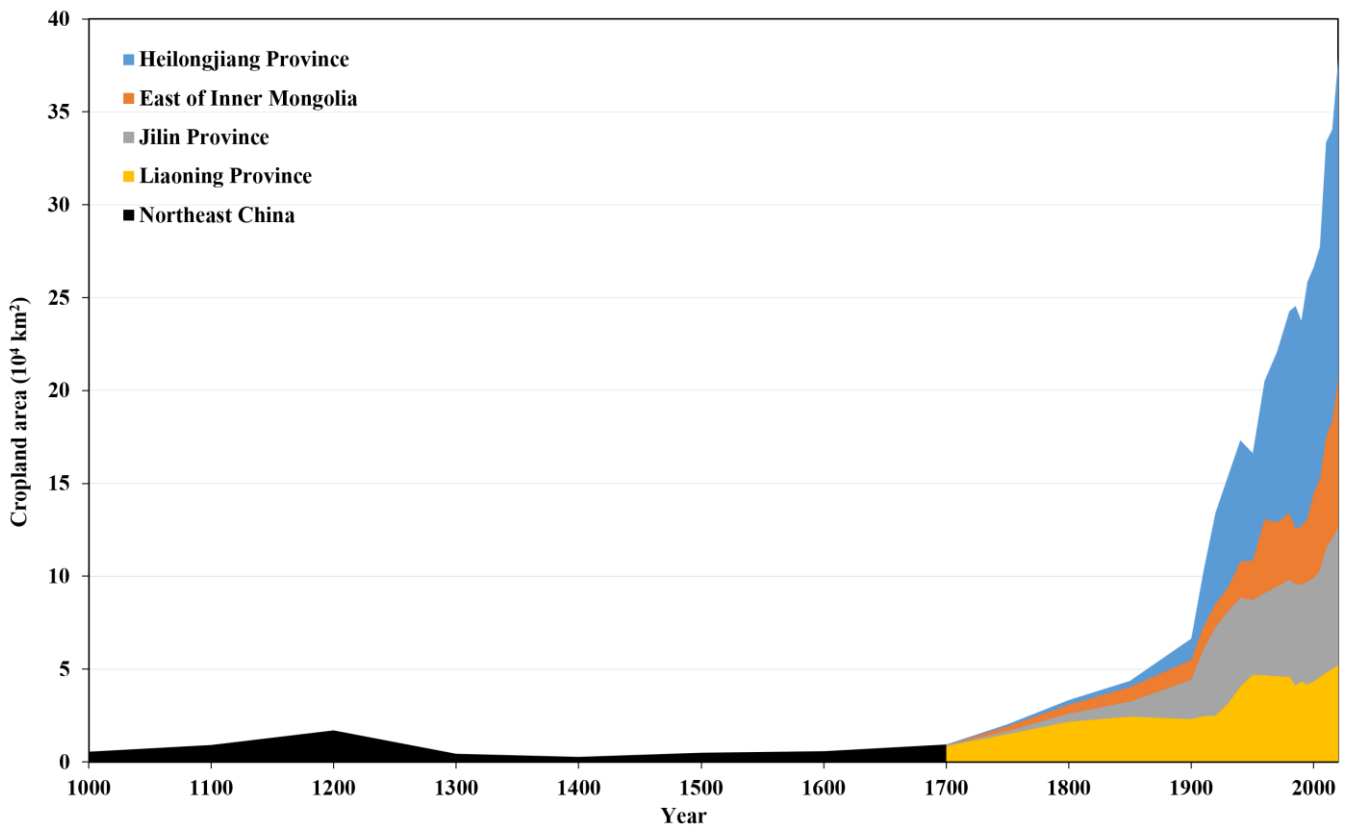
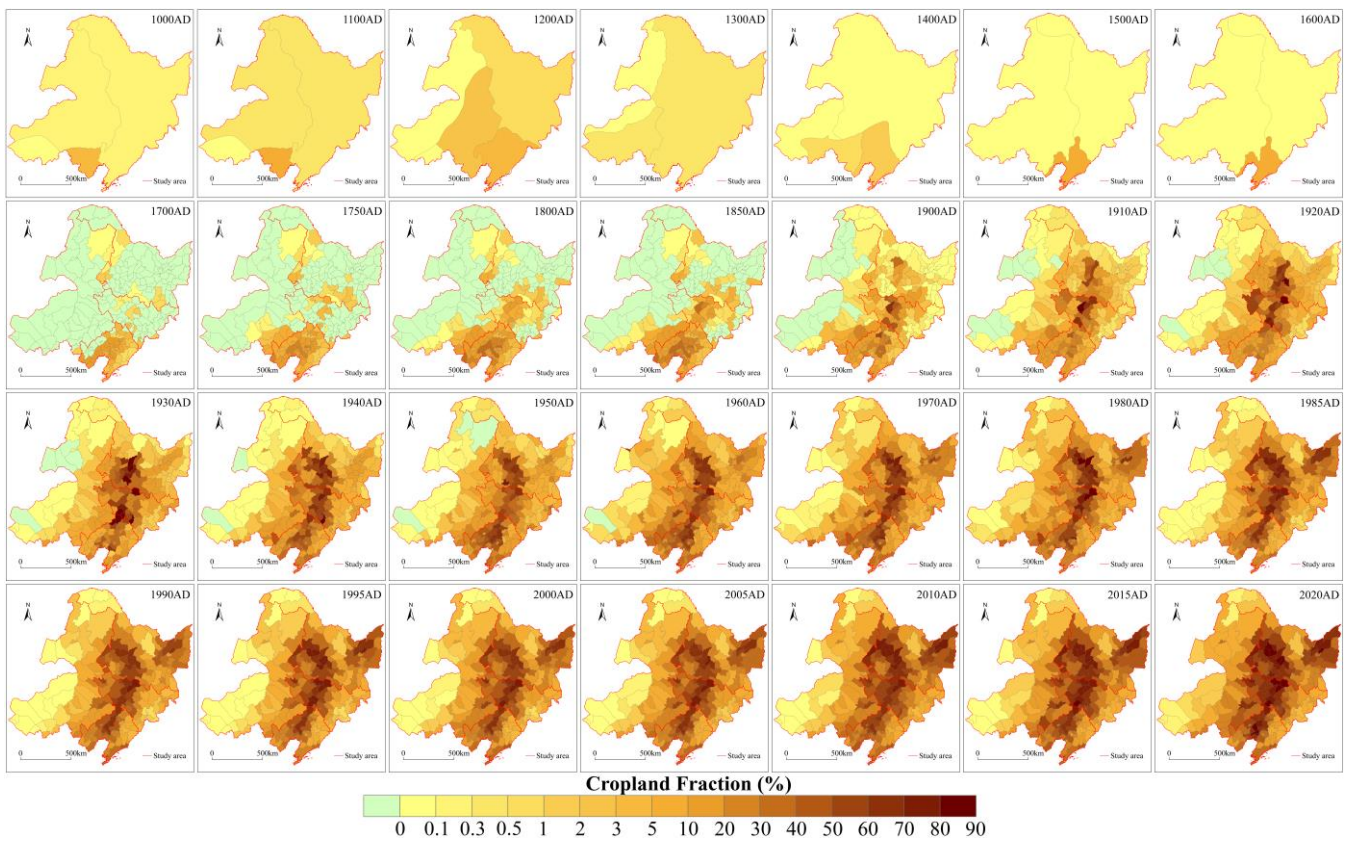


Figure 4: Changes in total cropland area in the Northeast China from 1000 to 2020.

3.2 Spatial patterns of cropland distribution in Northeast China over the past millennium

The changes in pattern of cropland in the Northeast China over the past millennium are shown in Figure 5. From 1000 to 1200, cropland in the study area had already reached a certain scale in spatial extent, mainly distributed in the Songliao Plain, especially in the southern part of the Liaohe Plain. The extent of cropland was roughly equivalent to the modern era. From 1300 to 1600, the main cultivation areas of cropland gradually receded southward to within the boundaries of Liaoning Province. From 1700 to 1850, cropland was mainly concentrated in the Liaoning Province. With the Qing government establishing military garrisons in the northern part of the Northeast China, farming areas were formed around these garrisons, and the farming area showed a trend of expanding northward. Due to the Qing government abandoning reclamation restrictive policies, from 1900 to 1950, the farming area gradually expanded to cover the entire region. Meanwhile, the cultivation intensity in the Hulunbuir City and Xilin Gol League of Inner Mongolia remained relatively low, influenced by war, leading to a slight decrease in the overall cropland fraction in 1950. After 1950, the farming area expanded rapidly and gradually formed a high cropland fraction agricultural zone with the Liaohe Plain, Songnen Plain, and Sanjiang Plain as its core.



424
425 **Figure 5: Changes in spatial patterns of cropland in the Northeast China from 1000 to 2020.**

426
427 **4 Discussion**

428 **4.1 Credibility assessment**

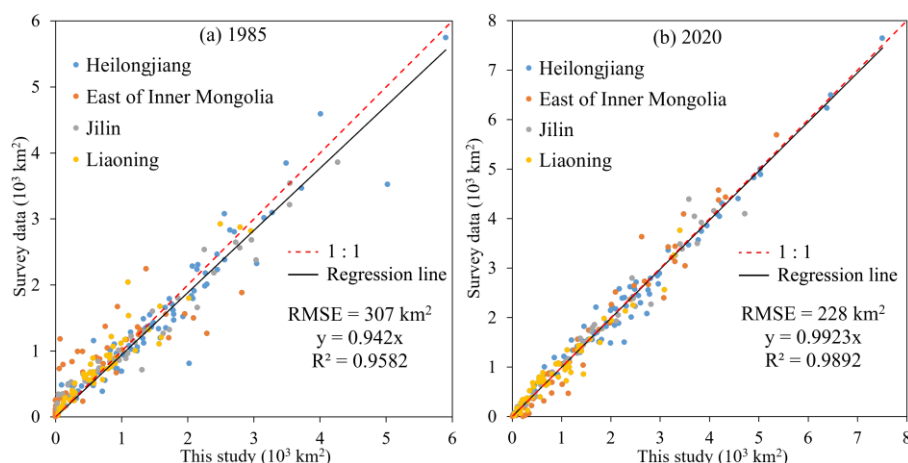
429 Based on the study of Fang et al. (2020), three methods including accuracy assessment, rationality assessment, and likelihood
430 assessment, can be used to assess the credibility of historical LUCC dataset. Regarding the likelihood assessment, in
431 reconstructing cropland area from 1985 to 2020, we selected eight RS products to assess the consistency. Based on the control
432 of cropland survey data, this study identified high-consistency and high-priority pixels as cropland pixels for this dataset and
433 evaluated and validated the accuracy of the integration results. Theoretically, compared with any single RS products used in
434 this study during this period, the total amount of cropland area in this study is relatively more accurate and the spatial
435 distribution is relatively more reasonable.

436 **4.1.1 Accuracy assessment**

437 The cropland data at lower spatial scales can be used to evaluate the accuracy of reconstructed cropland area. Due to the
438 availability of county-level cropland survey data, we selected the county-level first general land investigation at 1985 and the
439 county-level data from the third NLS at 2020 for comparison. As shown in Fig. 6, the determination coefficients between the
440 cropland area from this study and the cropland area from the survey data for 1985 and 2020 are 0.9582 and 0.9892 respectively.

441 This indicated that the overall accuracy of the reconstructed cropland area at county-level was relatively high, and our
442 constrained integration method that combines multisource cropland cover products with survey data can well match the spatial
443 distribution of cropland cover in Northeast China.

444 In addition, from 1985 to 2020, the identified high-consistency and high-priority pixels as cropland pixels based on
445 constrained integration method may lead to errors with survey data (Table S3). The relative errors between the cropland area
446 of this study and the cropland survey data for the period 1985 to 2020 as -1.35%, 4.02%, 5.17%, 1.10%, 0.21%, -1.93%, 0.25%
447 and 0.67%, respectively. The vast majority of errors are around 1%, with the larger errors are 4.02% and 5.17%, which indicates
448 that the reconstructed cropland area in this study is relatively accurate from 1985 to 2020.



449 **Figure 6: Correlation between the cropland data of this study and survey cropland data at county-level in the Northeast China in**
450 **1985 and 2020.**

452

453 4.1.2 Rationality assessment

454 Due to the unavailability of actual historical land cover data, we used the actual historical agricultural development of Northeast
455 China as a reference standard for rationality assessment. As one of the cases evaluating the distribution rationality of the
456 HYDE3.2 cropland cover in Northeast China over the past millennium, Fang et al. (2020) analyzed changes in the northern
457 boundary and spatial distribution of settlement relics in the Liao, Jin, Yuan, and Ming periods (916~1644), as well as changes
458 in the cumulative number of towns and spatial distribution of towns in the three provinces of Northeast China during the Qing
459 Dynasty (1644~1911). The unique development history of the Northeast China shown in this case is basically consistent with
460 the process of increase or decrease and spatial distribution of the total cropland area during the same period reconstructed by
461 this study, which reflects the rationality of this dataset.

462 In addition, this study attempts to briefly summarize the population changes, settlements changes (the settlement relics
463 and the administrative division points derived from Jia et al. (2018) and the Historical Atlas of China (Tan, 1982a; Tan, 1982b))
464 (Fig. S2), warfare, and land policies that may have influenced land cultivation in Northeast China during the Liao, Jin, Yuan,
465 and Ming periods (1000~1600). The population and settlements in Northeast China from 1000 to 1600 exhibited phase changes

466 of expansion-reduction-expansion, with possible reasons including the Liao and Northern Song Dynasties signed the
467 "*Chanyuan Alliance* (澶渊之盟)" in 1004 after war, the Jin and Southern Song Dynasties signed the "*Shaoxing Peace Treaty*
468 (绍兴和议)" in 1141 after war, the Jin and Southern Song Dynasties signed the "*Longxing Peace Treaty* (隆兴和议)" in 1164
469 after war. During the three treaties and related wars, both the Liao and Jin dynasties in the north benefited significantly. They
470 not only received reparations but also resettled large numbers of captives to the present-day Northeast China to engage in
471 agricultural and other productive activities. Historical records also indicate that the rulers of the Liao and Jin dynasties during
472 this period both attached much importance to agricultural production (Wu and Ge, 2022; Han, 1999; Toqto'A, 1974; Toqto'A,
473 1975).

474 From 1211, when Genghis Khan personally led the Mongol army to attack the Jin Dynasty, until 1233, the Mongols had
475 essentially gained control over the entire Northeast China. Using this region as a base, they also conducted war against Goryeo
476 (present-day Korean Peninsula), which lasted until 1259. From 1259 to 1287, the Mongols made several attempts to establish
477 governing institutions in Northeast China, but faced continuous rebellions. It wasn't until the Yuan Dynasty subdued the
478 rebellions and established the Liaoyang Province in 1287 that effective governance began in the Northeast China. However,
479 during this period, the region suffered from continuous warfare, significant population loss, and severe disruptions to
480 agricultural production (Xue, 2006, 2012). According to the *Dynastic History of Yuan Dynasty*, from 1294 to 1345, the Yuan
481 government provided relief to Liaoyang Province 40 times. Additionally, rebellions in the Northeast China persisted from 1343
482 onwards, only being effectively subdued the rebellions by 1362, just six years before the collapse of the Yuan Dynasty in 1368
483 (Song, 1976; Xue, 2006, 2012).

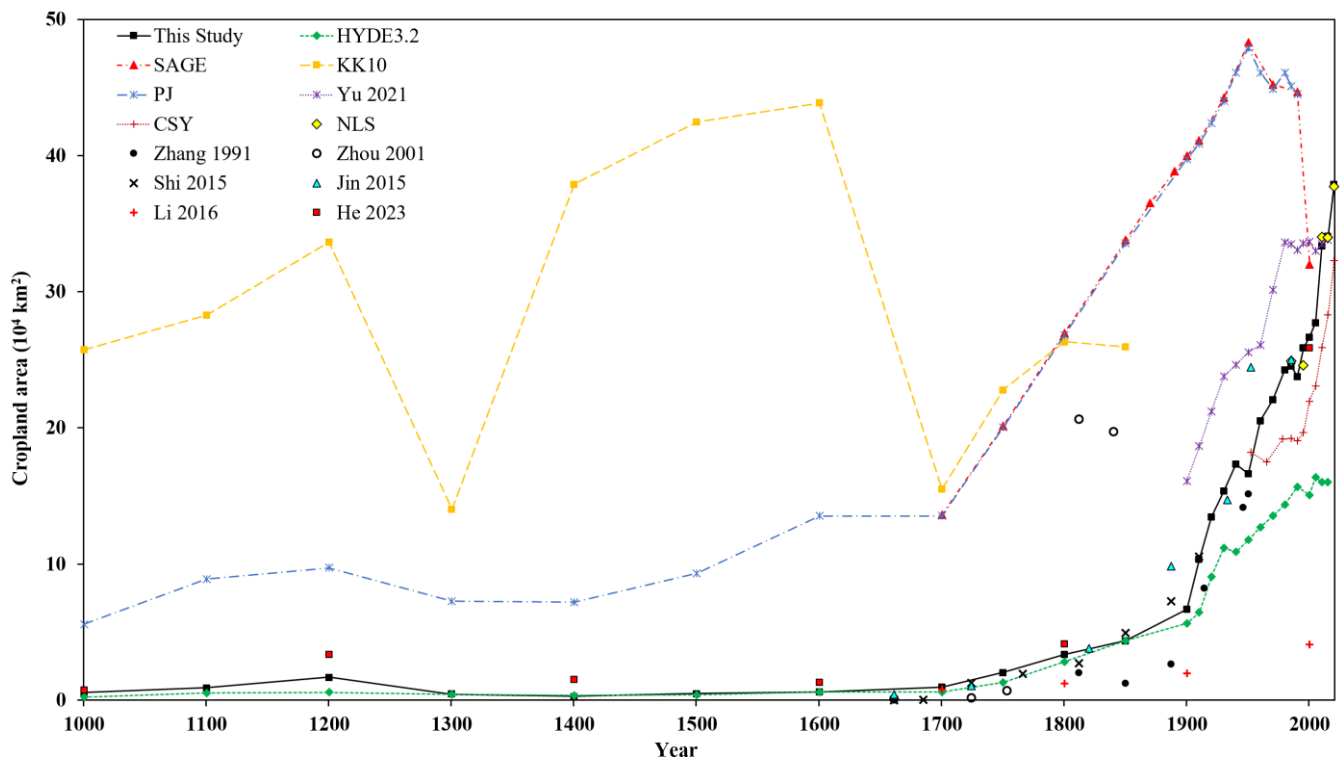
484 In 1368, the Ming Dynasty was established, and remnants of the Yuan Dynasty retreated to the northern grassland, known
485 as the Northern Yuan Dynasty (Tatar), which partly within our study area. It wasn't until 1389 that the Ming Dynasty established
486 the "*Uriyangqa three Commanderies* (兀良哈三卫)" in the region from present-day Qiqihar city to Baicheng city, gaining
487 certain practical control over the region. However, from 1399 to 1402, the Ming Dynasty faced the internal strife of the
488 "*Jingnan Campaign* (靖难之役)" weakening its influence over the Northeast China, allowing some ethnic minorities to further
489 occupy territories to the south. In 1409, the Ming Dynasty established the Dusi of Nuergan, reflecting their policy of
490 appeasement and assimilation towards ethnic minorities in the Northeast China. In 1449, the Ming Dynasty experienced the
491 "*Tumu Crisis* (土木之变)", prompting substantial efforts to fortify defensive structures. This also greatly strengthened the
492 defensive capabilities of the Ming Great Wall in the Northeast China and confined the major agricultural population and
493 agricultural areas of the Northeast China within the Dusi of Eastern Liao (south of the Ming Great Wall in the Northeast China).
494 This situation persisted until the Ming Dynasty's collapse in 1644 (Cao and Ge, 2022; Fan, 2015; Cao and Ge, 2005; Zhang,
495 1974). All these pieces of evidence contribute to the validation of the rationality of our dataset to a certain degree.

496

497 **4.2 Comparison with global historical LUCC datasets and previous studies**

498 To better showcase the achievements of this study, we chose to compare our results with widely used global historical LUCC
499 datasets (Fig. 7, Table S3): the History Database of the Global Environment (HYDE3.2) (Goldewijk et al., 2017), the
500 Sustainability and the Global Environment (SAGE) (Ramankutty et al., 2008; Ramankutty and Foley, 1999), the Kaplan and
501 Krumhardt 2010 (KK10) (Kaplan et al., 2011), and the Pongratz Julia (PJ) (Pongratz et al., 2008). Overall, the cropland area
502 curve of Northeast China in this study is generally between the HYDE3.2 dataset and the PJ dataset. The SAGE dataset, KK10
503 dataset, and PJ dataset consistently show significantly higher values than the results of this study throughout the past
504 millennium. It's worth noting that the KK10 dataset provides the combined area of cropland and pastureland, making it notably
505 larger than the results of this study compared to other datasets. The SAGE dataset, which obtained cropland area data using an
506 improved method in 2000, is relatively close to the results of this study. The curve of the PJ dataset is essentially consistent
507 with the SAGE dataset from 1700 to 1990 because the cropland data in the PJ dataset during this period are derived from the
508 SAGE dataset.

509 From the trend of the curve (Fig. 7), the HYDE3.2 dataset maintains a relatively low level of cropland area from 1000 to
510 1700. In comparison with this study, it fails to demonstrate the historical fact of cropland cultivation in the study area from
511 1000 to 1200. The HYDE3.2 dataset shows an increase in cropland area after 1700, with a growth rate similar to this study.
512 The growth rate significantly rises after 1900, but during this period, its growth rate is notably lower than in this study. The
513 SAGE dataset maintains a relatively high total cropland area and growth rate from 1700 to 1950. Subsequently, cropland area
514 starts to decline, approaching the results of this study in the year 2000. However, the total cropland area in the SAGE dataset
515 from 1700 to 2000 is significantly higher than the results of this study. The KK10 dataset exhibits drastic fluctuations from
516 1000 to 1850, with significant declines in the periods 1200 to 1300 and 1600 to 1700, placing the two points at the trough. For
517 the remaining periods, it maintains a growing trend, and the total area of cropland and pastureland in the KK10 dataset from
518 1000 to 1850 is significantly higher than the cropland area in this study. The PJ dataset shows a fluctuating upward trend from
519 1000 to 1700, with trends in growth and decline generally consistent with this study during this period. The minimum cropland
520 point is also around 1400, and after 1700, the total cropland area and growth rate in the PJ dataset are consistent with the SAGE
521 dataset. The cropland area in the PJ dataset is significantly higher than this study from 1000 to 1990.



522

523 **Figure 7: Comparison of total cropland area from global historical LUCC datasets, previous studies and this study in the Northeast**
 524 **China. The abbreviations used in the figure are as follows: HYDE3.2 refers to Goldewijk et al. (2017); SAGE refers to Ramankutty**
 525 **et al. (2008) and Ramankutty and Foley. (1999); KK10 refers to Kaplan et al. (2011); PJ refers to Pongratz et al. (2008); Yu 2021**
 526 **refers to Yu et al. (2021); CSY denotes the Chinese Statistical Yearbook (refer to provincial and prefectural statistical yearbook);**
 527 **NLS denotes the National Land Survey (1985 refer to the first general land investigation; 1995 refers to the first national land survey;**
 528 **2010 and 2015 refer to the second national land survey; 2020 refers to the third national land survey); Zhang 1991 refers to Zhang**
 529 **(1991); Zhou 2001 refers to Zhou (2001); Shi 2015 refers to Shi (2015); Jin 2015 refers to Jin et al. (2015); Li 2016 refers to Li et al.**
 530 **(2016); He 2023 refers to He et al. (2023).**

531

532 This study was compared the total cropland area with previous representative published studies in Northeast China (Fig.
 533 7, Table S3).

534 The data from Shi (2015) for 1661 and 1685 are significantly lower than this study, at these two time-points, Shi (2015)
 535 only had the data from Fengtian (roughly equivalent to Liaoning Province). Although the data from Shi (2015) for 1724
 536 included the total area for Heilongjiang, Jilin, and Fengtian, the territorial scope of Heilongjiang and Jilin during this period
 537 was larger than that of present-day Heilongjiang and Jilin provinces. We did not exclude the cropland area according to the
 538 proportion of these territory outside present-day China. Additionally, there were 15.35, 15.35, and 17.35 million Qing *Mu*
 539 (9431 km², 9431 km², and 10660 km²) of banner cropland at these three time-points, mainly distributed in Zhili (partly within
 540 our study area) and various parts of Northeast China, which could not be accurately divided. Therefore, we did not include the
 541 banner cropland for these three time-points. For the Mongolia in 1766, 1812, 1850, 1887, and 1911 from Shi (2015), we
 542 converted the data based on the area proportion of the Qing Dynasty Mongolia within our study area, which is 41.58%.

543 The data from Jin et al. (2015) closely matches this study growth trend. Both studies acknowledge that the 1985 land

544 survey data is relatively accurate, resulting in no significant differences at this point. In Jin et al. (2015), the data in the Inner
545 Mongolia in 1661 is missing, and for subsequent time-points, we calculated the data based on the area proportion of the East
546 of Inner Mongolia (within our study area), which is 55.26%. The data in 1661, 1724, 1820, 1887, 1933, and 1952 from Jin et
547 al. (2015) is similar to this study. The main reason for the difference in cropland area between the two studies may be due to
548 the specific data source and data adjustment methods.

549 The data from He et al. (2023) closely matches this study growth trend. It should be noted that, for clearer comparison
550 with our study, we selected standard time-points every 200 years from 1000 to 2000 on the cropland area curve from He et al.
551 (2023). Similarly, we calculated the cropland area in the East of Inner Mongolia (within our study area) based on the proportion
552 of 55.26%. In He et al. (2023), the data from 1000 to 1800 is slightly higher than this study, possibly because of the different
553 methods for reconstruct the cropland area based on the population and the different proxy indicators used by the two studies
554 during this period.

555 Similar to the comparison with He et al. (2023), when selecting the CHCD data from Li et al. (2016) for comparison, we
556 chose standard time-points every 100 years from 1700 to 2000 on the cropland area curve for Inner Mongolia from CHCD
557 data, and calculated the area for the East of Inner Mongolia based on 55.26%. The CHCD data for Heilongjiang, Jilin, and
558 Liaoning province is consistent with our study (Ye et al., 2009), however, this study corrected Ye's data as explained earlier
559 (Table S1). The difference in cropland area for the East of Inner Mongolia between the two studies may be due to the calculation
560 of cropland area based on the proportion of 55.26%, which may not align with the actual historical agricultural development
561 of Inner Mongolia.

562 For the sake of clear comparison, we selected standard time points every decade from 1900 to 1980, and every five years
563 from 1985 to 2015 from Yu et al. (2021). The difference between the two studies in 2015 is minimal, as both studies
564 acknowledge the NLS data is relatively accurate. The main reason for the difference in cropland area between the two studies
565 may be due to the different reconstruction methods. In Yu et al. (2021), the officially released NLS data in 2017 (cropland area
566 in 2016) is used as the benchmark data, and an assumption was made that this most recent data is the most reliable. Then
567 calculated the national cropland area by using the NLS data in 2017 as the baseline and adjusted using the interannual variation
568 information of cropland derived from various sources. Due to the cropland area difference between the national total and the
569 sum of the provincial, a proportional adjustment was applied to match the provincial to the national total. In this study, three
570 times NLS data were adopted, we assumed that the cropland survey data is the most reliable, then corrected the statistical data
571 through the correlation coefficients between the statistical and the survey data in different periods to obtain the cropland area
572 for the time-points without survey data.

573 The data from Zhang (1991) consistently shows lower values compared to this study across all time points. The differences
574 may arise because the lack of data in Inner Mongolia for all periods except 1949 from Zhang (1991). Both studies agree that

575 national statistical data is reliable for 1950s, the data from Zhang (1991) is slightly underestimates compared to our study,
576 likely due to the calculation of cropland area based on the proportion of 55.26% in the East of Inner Mongolia.

577 The data from Zhou (2001) shows lower values compares to this study in 1661, 1724, and 1753. The differences may
578 arise because the lack of data in Heilongjiang, Jilin province, and Inner Mongolia in these periods. Conversely, in 1812 and
579 1840, the data from Zhou (2001) is significantly exceeds to our study. The differences may arise because the assumption of
580 the cropland. In Zhou (2001), an important assumption is that the northern territorial boundaries were much larger than today,
581 then the cropland area of Heilongjiang, Jilin, and Liaoning province in 1952 were used instead of the cropland area in 1812
582 and 1840. This assumption may contradict the actual historical agricultural development of Northeast China.

583 **4.3 Spatial distribution of cropland cover compared with HYDE3.2 dataset**

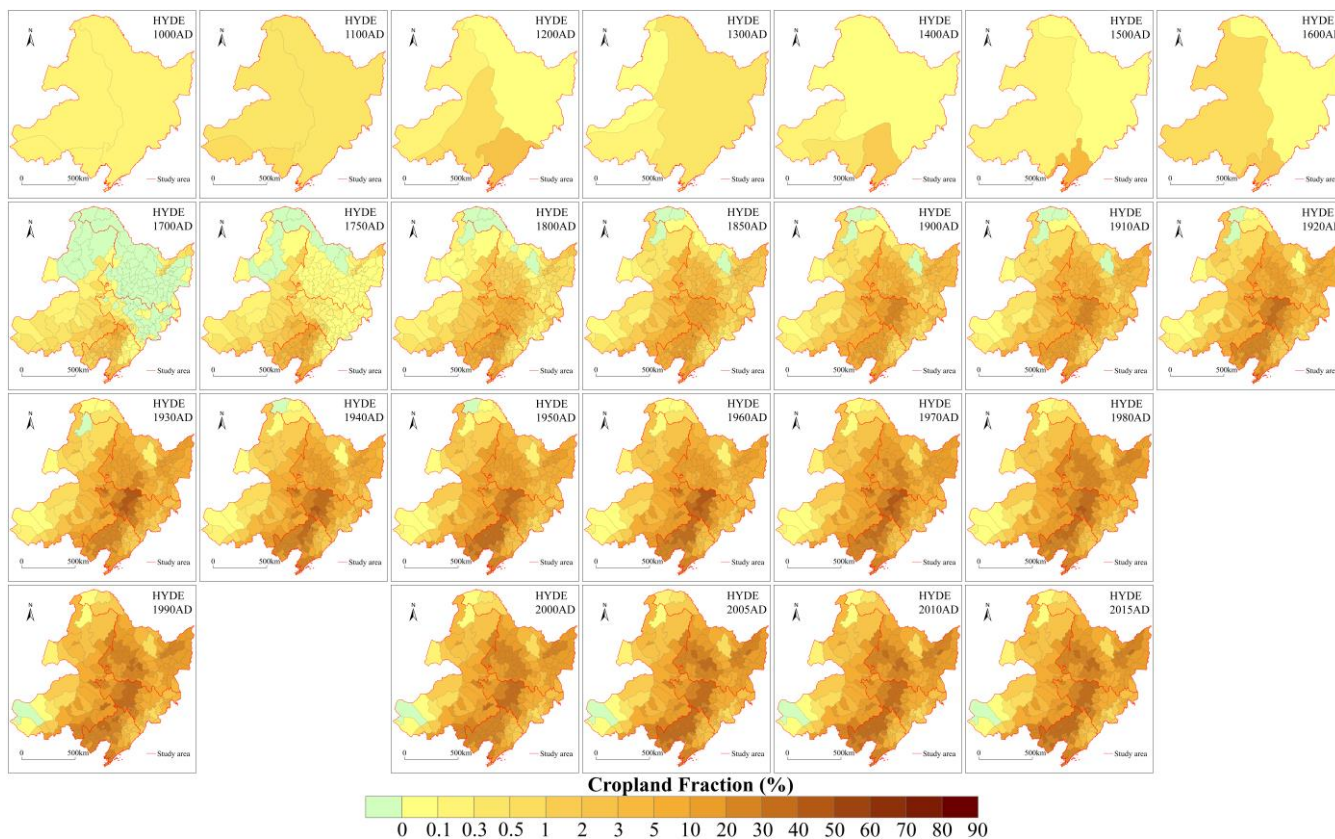
584 We acknowledged that there is no more credible cropland area data at the global scale than HYDE up to now. Compared to
585 this study, the HYDE3.2 dataset shows relative differences ratio (RD) in total cropland area for the period 1000 to 1600 as -
586 82.92%, -52.52%, -100.45%, -5.32%, 17.42%, -29.34%, and 0.55%, respectively (Fig. 8~9). The relative differences ratio (RD)
587 as shown in Equation (4):

$$588 \text{RD} = \frac{C_H(y) - C_T(y)}{(C_H(y) + C_T(y))/2} \times 100\% , \quad (4)$$

589 where $C_H(y)$ represents the total cropland area from HYDE3.2 for year y , and $C_T(y)$ represents the total cropland area from
590 this study for year y .

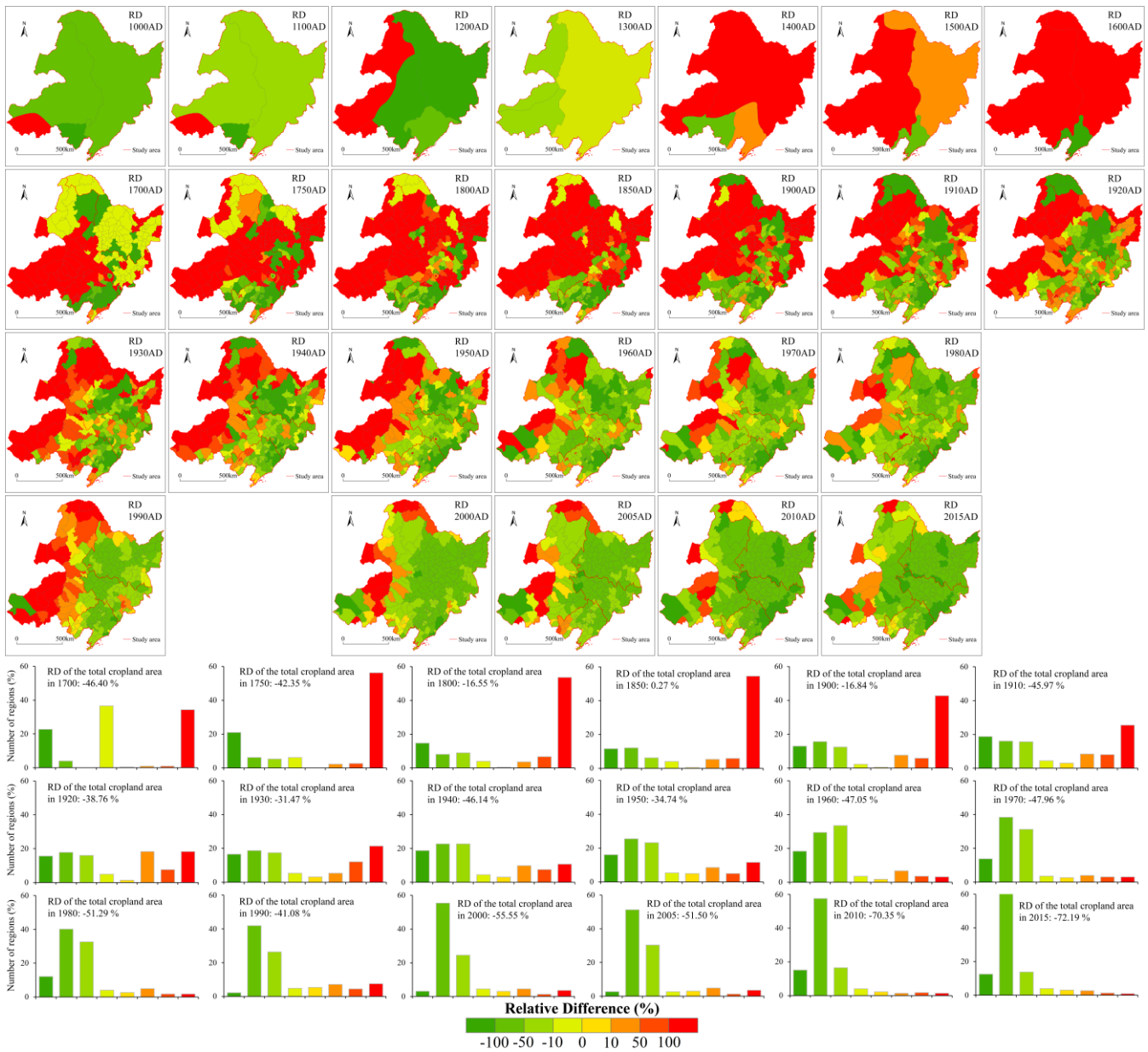
591 Compared to this study, except for the years 1100 and 1300, where the absolute values of RD in most provinces within
592 the study area did not exceed 50%, for other years, most provinces showed relatively large RD. In the years 1000 and 1100,
593 except for certain areas in Xilin Gol League where the HYDE3.2 dataset showed more cropland area, the rest of the regions
594 generally had less cropland area than this study. In 1200, the HYDE3.2 dataset showed more cropland area in the western
595 region, while the opposite was observed in the eastern region. In 1300, the HYDE3.2 dataset indicated less cropland area in
596 the entire region. From 1400 to 1600, the HYDE3.2 dataset showed more cropland area in the northern region. As the scope
597 of the Dusi of Eastern Liao reduced, this study's cropland area in this region significantly exceeded the HYDE3.2 dataset. In
598 1700, both the HYDE3.2 dataset and this study indicated that most counties in Heilongjiang and Jilin provinces, as well as the
599 northeastern part of Inner Mongolia, had no cropland (Fig. 5, Fig. 8). However, the HYDE3.2 dataset showed that during this
600 period, a considerable area of cropland existed in most regions of Inner Mongolia and the Sanjiang Plain, leading to 34.38%
601 of county-level RDs being greater than 100% (Fig. 9). From 1750 to 1850, the HYDE3.2 dataset showed that the expansion
602 of cropland cultivation gradually extended northward to cover the entire region (Fig. 8). This contradicts the areas without
603 cropland caused by the abandoning reclamation restrictive policies of the Qing government during this period. Additionally,
604 during this period, in the counties which both datasets considered with cropland, this study found that, except for a few counties

605 where cropland area was less than the HYDE3.2 dataset, most counties had significantly more cropland area in this study.
 606 During this period, over half of the counties in the study area had RDs greater than 100%. From 1900 to 1950, as the abandoning
 607 reclamation restrictive policies, this study observed a decreasing trend in cropland fraction from the center to the periphery in
 608 the study area (Fig. 5). Compared to the HYDE3.2 dataset, counties with RD greater than 100% gradually decreased (Fig. 9).
 609 Furthermore, during this period, in most areas of the Songnen Plain and the Liaohe Plain, this study's cropland area was
 610 significantly greater than the HYDE3.2 dataset. After 1950, the RD for each county in the study area gradually decreased and
 611 concentrated in the (-100%, -10] range (Fig. 9), indicating that the cropland area in most counties in this study was significantly
 612 greater than the HYDE3.2 dataset.



613
 614 **Figure 8: Changes in spatial patterns of cropland of HYDE3.2 dataset in the Northeast China from 1000 to 2015.**

615



616

617

Figure 9: Comparison of the spatial distribution of cropland area between HYDE3.2 and this study in the Northeast China.

618

619 4.4 Uncertainty analysis

620

In this study, the uncertainty mainly consisted in two aspects: the definition and selection of data, the application of methods.

621

Regarding the data aspect: (1) In this study, the definition of cropland before 1950 is: the sum of arable land and land under

622

permanent crops, and the temporary changes in land use and fallow land during historical periods were not considered. The

623

cropland area for 1950 and later are basically consistent with the identification rules in the NLS. Although the temporary

624

changes in land use and fallow land during historical periods, this may still result in our reconstruction slightly less cropland

625

than actual historical period.

626

(2) Due to the completeness of historical documents, the reconstruction results of cropland for seven time points from

627

1000 to 1600 in this study are at the provincial-level, which may not finely reflect the spatiotemporal characteristics of cropland.

628 Especially between 1000 and 1300, the results may lead readers to mistakenly believe that cropland were evenly distributed
629 across the entire Northeast China. However, based on the distribution of settlement relics during this period, cropland may
630 mainly distribute on the Liaohe Plain and on the southern part of the Songnen Plain, then reduced southward into Liaoning
631 Province.

632 (3) The two proxy indicators of 14 *Mu* (0.93 hm², the average annual potential cropland area per Man of the agricultural
633 population) and 2 *Mu* (0.13 hm², the average cropland area per household in the nonagricultural population) from 1000 to 1600
634 may lead to inaccuracies in cropland estimation. The reasons for using population to reconstruct cropland during this period
635 have been detailed in the previous section, necessitating further analysis and clarification of the corresponding cropland-related
636 indicators.

637 Firstly, the conclusion of 14 *Mu* per Man for agricultural population during the Liao and Jin Dynasties (1000~1200) is
638 primarily derived from historical records in the Jin Dynasty (1200) and the relationship between population and cropland in
639 the early Qing Dynasty (1661~1680) (Jia et al., 2023). There are two reasons why 14 *Mu* was used in the Yuan and Ming
640 Dynasties (1300~1600): one reason is the agricultural household size and the ratios of Man in agricultural household in
641 Northeast China during the Yuan and Ming Dynasties (1300~1600) are closer to those of the Liao and Jin Dynasties
642 (1000~1200) (Table 1). And the per capita cropland area owned by agricultural population in the Liao-Jin-Yuan-Ming periods
643 (1000~1600) consistently ranged between 4 and 5 *Mu* (0.27~0.33 hm²), slightly higher than the subsistence level of 3 *Mu* per
644 capita in previous studies for the same historical period in this region (Ye et al., 2009; Fang et al., 2006; Shi, 1990), which is
645 relatively reasonable. The second reason is that there were no significant changes in agricultural production technology in
646 Northeast China during the Liao-Jin-Yuan-Ming periods (1000~1600), and the population declined significantly compared
647 with the Liao and Jin Dynasties (1000~1200) due to factors such as warfare. However, considering the social stability at
648 standard time-points during the Yuan and Ming Dynasties (1300~1600), the strong willingness of the agricultural population
649 towards cultivation, and the limitations of individual cultivation capabilities, the cropland from the Liao and Jin Dynasties
650 could be relatively easily inherited and reclaimed by descendants.

651 Secondly, Similar to the agricultural population, considering the non-agricultural household size, stable agricultural
652 production technology, the historical inheritance of most ethnic groups, this study continues to use 2 *Mu* as the calculation
653 indicator of non-agricultural population in the Yuan and Ming Dynasties (1300~1600) (Cong, 1993a; Cong, 1993b; Wu and
654 Ge, 2005a; Cao and Ge, 2005b; Liu et al., 2016).

655 Regarding the method aspect: (1) From 1700 to 1980, cropland areas at multiple time points in this study were derived
656 through linear interpolation and polynomial curve fitting. Although we have fully considered historical facts and other research
657 conclusions (Fang et al., 2020; Ye et al., 2009; Fang et al., 2005) when selecting the interpolation time points, 1860 was chosen
658 as the dividing point between slow growth and rapid growth. This method, compared to data recorded at each specific historical

659 point, may affect the accuracy of the value at those standard time points.

660 (2) From 1700 to 1980, the county-level administrative boundaries in the published data used in this study differ from the
661 modern county-level administrative boundaries used in this study. Especially in the CNEC data (Ye et al., 2009) in 1683, 1735
662 and 1780, there is county-level in Liaoning province, Assistant Governorate Jurisdiction (prefecture-level) in Heilongjiang and
663 Jilin province. This would result in counties belonging to different Assistant Governorate Jurisdictions in present-day having
664 the same cropland fraction. This problem is difficult to correct further because the lowest administrative level in Northeast
665 China available in historical data during this period is Assistant Governorate Jurisdiction (prefecture-level).

666 (3) From 1985 to 2020, the land survey data utilized in this dataset might exhibit uncertainties in early cropland data due
667 to backward technology and other factors. Additionally, the use of a uniform correlation coefficient to correct the cropland
668 statistics data for the entire Northeast China may affect the accuracy of the cropland area in localized areas, this may lead to a
669 lower cropland area at previous time-points. To mitigate the impact of these uncertainties on our dataset during this period,
670 this study mainly adopts two methods: Firstly, this study mainly selects the standard time-points data after the nationwide
671 surveys, avoiding the use of annual land change survey data. For instance, the cropland area in 1985 in this dataset is based on
672 the first general land investigation around 1985; the cropland area in 1995 is based on the first NLS's standard time-point data
673 on October 31, 1996; the cropland area in 2010 is based on the second NLS's standard time-point data on December 31, 2009;
674 and the cropland area in 2020 is based on the third NLS's standard time-point data on December 31, 2019. Secondly, this study
675 uses correlation coefficients to correct the statistical data by category and time point. For instance, the average correlation
676 coefficient of the second and third NLSs with corresponding statistical data is used to correct the statistical data for the 1990,
677 2000, and 2005; the correlation coefficient of the 1985 first general land investigation with corresponding statistical data is
678 used to correct the statistical data for the 1950~1980.

679

680 **5 Data availability**

681 All cropland data reconstructed in this study are publicly available at <https://doi.org/10.6084/m9.figshare.25450468.v2> (Jia,
682 2024).

683

684 **6 Conclusion**

685 Based on historical documents, proxy data such as population data, revised published results, remote sensing data products,
686 statistical data, and survey data, and utilizing a series of data processing methods, as well as accuracy and rationality assessment
687 methods, we established a 28 time-points cropland area dataset in Northeast China at provincial-level and county-level spatial

688 resolutions from 1000 to 2020. Reconstruction results indicate that cropland area in Northeast China grew slowly before 1850
689 and experienced rapid expansion after 1850, maintaining this growth trend until 2020. This dataset illustrates the characteristics
690 of cropland changes in Northeast China over the past millennium, especially in the past 300 years. Between 1000 and 1200,
691 the extent of cropland was roughly equivalent to the modern era. Subsequently, until 1850, the cropland was mainly
692 concentrated in the Liaoning Province. However, with the Qing government establishing military garrisons in the northern part
693 of the Northeast China, farming areas was formed around these garrisons from 1700 to 1850. With the implementation of the
694 immigration and cultivation policy in the latter half of the 19th century, the spatial pattern of cropland coverage in Northeast
695 China changed significantly after 1850, with agricultural zones rapidly expanding across the entire region. After 1950, the
696 expansion of high cropland fraction agricultural zones in Northeast China became more pronounced, gradually forming core
697 areas with high cropland fraction in the Liaohe Plain, Songnen Plain, and Sanjiang Plain.

698 Despite the fact that the cropland area change dataset in this study is presented at the provincial-level and county-level,
699 the dataset we reconstructed based on historical records at 28 time points can be approximated as “truth value”. This dataset
700 provides crucial support for the long-term land use changes in the Northeast China. In the future, we will further investigate
701 gridded cropland allocation methods based on the historical cultivation process in the Northeast China, aiming to better serve
702 research such as carbon emission, climate data construction, climate-ecosystem modeling and the conservation and utilization
703 of black soil, etc.

705

706 **Author contributions.** RJ, XF and Yu Y designed this work. RJ wrote the manuscript. XF and Yu Y provided suggestions on
707 methodology. Yu Y and Yundi Y developed the dataset. All the authors contributed to the review of the manuscript.

708

709 **Competing interests.** The authors declare that they have no conflict of interest.

710

711 **Financial support.** This research has been supported by the National Key R&D Program of China (grant no.
712 2021YFD1500704), and the Fund of the China Scholarship Council (grant no. 202306040062).

713

714

715 **References**

- 716 Arneth, A., Sitch, S., Pongratz, J., Stocker, B. D., Ciais, P., Poulter, B., Bayer, A. D., Bondeau, A., Calle, L., Chini, L. P., Gasser,
717 T., Fader, M., Friedlingstein, P., Kato, E., Li, W., Lindeskog, M., Nabel, J. E. M. S., Pugh, T. A. M., Robertson, E., Viovy,
718 N., Yue, C., and Zaehle, S.: Historical carbon dioxide emissions caused by land-use changes are possibly larger than
719 assumed, *Nat. Geosci.*, 10, 79-84, <https://doi.org/10.1038/NGEO2882>, 2017.
- 720 Bai, S., Shuwen, Z., and Yangzhen, Z.: Digital rebuilding of lucc spatial-temporal distribution of the last 100 years: taking
721 dorbod mongolian autonomous county in daqing city as an example, *Acta Geographica Sinica*, 62, 427-436, 2007.
- 722 Cao, B., Yu, L., Li, X., Chen, M., Li, X., Hao, P., and Gong, P.: A 1 km global cropland dataset from 10 000 bce to 2100 ce,
723 *Earth Syst. Sci. Data*, 13, 5403-5421, <https://doi.org/10.5194/essd-13-5403-2021>, 2021.
- 724 Chen, J., Chen, J., Liao, A., Cao, X., Chen, L., Chen, X., He, C., Han, G., Peng, S., Lu, M., Zhang, W., Tong, X., and Mills, J.:
725 Global land cover mapping at 30 m resolution: a pok-based operational approach, *Isprs-J. Photogramm. Remote Sens.*,
726 103, 7-27, <https://doi.org/10.1016/j.isprsjprs.2014.09.002>, 2015.
- 727 Dickinson, R. E.: Global change and terrestrial hydrology - a review, *Tellus Ser. B-Chem. Phys. Meteorol.*, 43A-B, 176-181,
728 <https://doi.org/10.1034/j.1600-0870.1991.00015.x>, 1991.
- 729 Ellis, E. C., Gauthier, N., Goldewijk, K. K., Bird, R. B., Boivin, N., Diaz, S., Fuller, D. Q., Gill, J. L., Kaplan, J. O., Kingston,
730 N., Locke, H., Mcmichael, C. N. H., Ranco, D., Rick, T. C., Rebecca Shaw, M., Stephens, L., Svenning, J. C., and Watson,
731 J. E. M.: People have shaped most of terrestrial nature for at least 12,000 years, *Proceedings of the National Academy of*
732 *Sciences - PNAS*, 118, 1, <https://doi.org/10.1073/pnas.2023483118>, 2021. Fang, X., Zhao, W., Zhang, C., Zhang, D., Wei,
733 X., Qiu, W., and Ye, Y.: Methodology for credibility assessment of historical global lucc datasets, *Science China Earth*
734 *Sciences*, 1013-1025, <https://doi.org/10.1007/s11430-019-9555-3>, 2020.
- 735 Foley, J. A., Defries, R., Asner, G. P., Barford, C., Bonan, G., Carpenter, S. R., Chapin, F. S., Coe, M. T., Daily, G. C., Gibbs,
736 H. K., Helkowski, J. H., Holloway, T., Howard, E. A., Kucharik, C. J., Monfreda, C., Patz, J. A., Prentice, I. C.,
737 Ramankutty, N., and Snyder, P. K.: Global consequences of land use, *Science*, 309, 570-574,
738 <https://doi.org/10.1126/science.1111772>, 2005.
- 739 Friedlingstein, P., Jones, M. W., Andrew, R. M., Bakker, D. C. E., Hauck, J., Landschützer, P., Luijkx, I. T., Peters, G. P., Peters,
740 W., Pongratz, J., Sitch, S., Ciais, P., Jackson, R. B., Alin, S. R., Anthoni, P., Barbero, L., Bates, N. R., Becker, M., Bellouin,
741 N., Decharme, B., Bopp, L., Brasika, I. B. M., Cadule, P., Chamberlain, M. A., Chandra, N., Chau, T., Chini, L. P., Dou,
742 X., Enyo, K., Evans, W., Falk, S., Feng, L., Gasser, T., Ghattas, J., Gkritzalis, T., Grassi, G., Gruber, N., Gürses, Ö., Harris,
743 I., Hefner, M., Hurtt, G. C., Iida, Y., Jacobson, A. R., Jain, A., Jarníková, T., Jersild, A., Jin, Z., Joos, F., Kato, E., Keeling,
744 R. F., Kennedy, D., Klein Goldewijk, K., Knauer, J., Körtzinger, A., Lan, X., Lefèvre, N., Li, H., Ma, L., Marland, G.,
745 Mayot, N., Mcguire, P. C., Meyer, G., Morgan, E. J., Munro, D. R., Nakaoka, S., Niwa, Y., O'Brien, K. M., Olsen, A.,

746 Ono, T., Paulsen, M., Pierrot, D., Pocock, K., Poulter, B., Rehder, G., Robertson, E., Rosan, T. M., Schwinger, J., Séférian,
747 R., Smallman, T. L., Smith, S. M., Sospedra-Alfonso, R., Sun, Q., Sutton, A. J., Sweeney, C., Tans, P. P., Tilbrook, B.,
748 Tsujino, H., Tubiello, F., van der Werf, G. R., van Ooijen, E., Wanninkhof, R., Watanabe, M., Wimart-Rousseau, C., Yang,
749 D., Yang, X., Yuan, W., Yue, X., Zaehle, S., Zeng, J., and Zheng, B.: Global carbon budget 2023, *Earth Syst. Sci. Data*,
750 15, 5301-5369, <https://doi.org/10.5194/essd-15-5301-2023>, 2023.

751 Gaillard, M., Morrison, K. D., Madella, M., and Whitehouse, N.: Past land-use and land-cover change: the challenge of
752 quantification at the subcontinental to global scales, <https://doi.org/10.22498/pages.26.1.3>, 2018.

753 Godfray, H. C. J., Beddington, J. R., Crute, I. R., Haddad, L., Lawrence, D., Muir, J. F., Pretty, J., Robinson, S., Thomas, S.
754 M., and Toulmin, C.: Food security: the challenge of feeding 9 billion people, *Science*, 327, 812-818,
755 <https://doi.org/10.1126/science.1185383>, 2010.

756 Goldewijk, K. K., Beusen, A., Doelman, J., and Stehfest, E.: Anthropogenic land use estimates for the holocene - hyde 3.2,
757 *Earth Syst. Sci. Data*, 9, 927-953, <https://doi.org/10.5194/essd-9-927-2017>, 2017.

758 Gong, P., Wang, J., Le Yu, Zhao, Y., Zhao, Y., Liang, L., Niu, Z., Huang, X., Fu, H., Liu, S., Li, C., Li, X., Fu, W., Liu, C., Xu,
759 Y., Wang, X., Cheng, Q., Hu, L., Yao, W., Zhang, H., Zhu, P., Zhao, Z., Zhang, H., Zheng, Y., Ji, L., Zhang, Y., Chen, H.,
760 Yan, A., Guo, J., Yu, L., Wang, L., Liu, X., Shi, T., Zhu, M., Chen, Y., Yang, G., Tang, P., Xu, B., Giri, C., Clinton, N.,
761 Zhu, Z., Chen, J., and Chen, J.: Finer resolution observation and monitoring of global land cover : first mapping results
762 with landsat tm and etm+ data, *Int. J. Remote Sens.*, 34, 2607-2654, <https://doi.org/10.1080/01431161.2012.748992>, 2013.

763 Gortan, M., Testa, L., Fagiolo, G., and Lamperti, F.: A unified dataset for pre-processed climate indicators weighted by gridded
764 economic activity, *Sci. Data*, 11, 533, <https://doi.org/10.1038/s41597-024-03304-1>, 2024.

765 He, F., Yang, F., Zhao, C., Li, S., and Li, M.: Spatially explicit reconstruction of cropland cover for china over the past
766 millennium., *Science China Earth Sciences*, 66, 111-128, <https://doi.org/10.1007/s11430-021-9988-5>, 2023.

767 He, F., Li, M., and Li, S.: Reconstruction of Lu-level cropland areas in the Northern Song Dynasty (AD976-1078), *Acta*
768 *Geographica Sinica*, 606-618, <https://doi.org/10.1007/s11442-017-1395-3>, 2017.

769 Huang, X., Ibrahim, M. M., Luo, Y., Jiang, L., Chen, J., and Hou, E.: Land Use Change Alters Soil Organic Carbon: Constrained
770 Global Patterns and Predictors, *Earth's Future*, 12, n/a, <https://doi.org/10.1029/2023EF004254>, 2024.

771 Hurtt, G. C., Chini, L., Sahajpal, R., Frohling, S., Bodirsky, B. L., Calvin, K., Doelman, J. C., Fisk, J., Fujimori, S., Goldewijk,
772 K. K., Hasegawa, T., Havlik, P., Heinemann, A., Humpenöder, F., Jungclaus, J., Kaplan, J. O., Kennedy, J., Krisztin, T.,
773 Lawrence, D., Lawrence, P., Ma, L., Mertz, O., Pongratz, J., Popp, A., Poulter, B., Riahi, K., Shevliakova, E., Stehfest,
774 E., Thornton, P., Tubiello, F. N., Vuuren, D. P. V., Zhang, X., and Pacific Northwest National Lab. Pnnl, R. W. U. S.:
775 Harmonization of global land use change and management for the period 850–2100 (luh2) for cmip6, *Geosci. Model Dev.*,
776 13, 5425-5464, <https://doi.org/10.5194/gmd-13-5425-2020>, 2020.

777 Ito, A. and Hajima, T.: Biogeophysical and biogeochemical impacts of land-use change simulated by miroc-es2l, *Prog. Earth*
778 *Planet. Sci.*, 7, 1-15, <https://doi.org/10.1186/s40645-020-00372-w>, 2020.

779 Jia, D., Li, Y., and Fang, X.: Complexity of factors influencing the spatiotemporal distribution of archaeological settlements in
780 northeast China over the past millennium, *Quat. Res.*, 413-424, 2018.

781 Jia, R., Fang, X., and Ye, Y.: Gridded reconstruction of cropland cover changes in northeast china from ad 1000 to 1200, *Reg.*
782 *Envir. Chang.*, 23, 128, <https://doi.org/10.1007/s10113-023-02118-y>, 2023.

783 Jia, R., Fang, X., Yang, Y., Yokozawa, M., and Ye, Yu.: A 28 time-points cropland area change dataset in Northeast China from
784 1000 to 2020. figshare. Dataset. <https://doi.org/10.6084/m9.figshare.25450468.v2>, 2024.

785 Jin, X., Cao, X., Du, X., Yang, X., Bai, Q., and Zhou, Y.: Farmland dataset reconstruction and farmland change analysis in
786 China during 1661-1985, *Acta Geographica Sinica*, 1058-1074, 2015.

787 Kalnay, E. and Cai, M.: Impact of urbanization and land-use change on climate, *Nature*, 423, 528-531,
788 <https://doi.org/10.1038/nature01675>, 2003.

789 Kaplan, J. O., Krumhardt, K. M., Ellis, E. C., Ruddiman, W. F., Lemmen, C., and Goldewijk, K. K.: Holocene carbon emissions
790 as a result of anthropogenic land cover change, *The Holocene*, 21, 775-791, <https://doi.org/10.1177/0959683610386983>,
791 2011.

792 Karra, K., Kontgis, C., Statman-Weil, Z., Mazzariello, J. C., Mathis, M., and Brumby, S. P.: Global land use/land cover with
793 sentinel 2 and deep learning, in: 2021 IEEE International Geoscience and Remote Sensing Symposium IGARSS, The
794 Institute of Electrical and Electronics Engineers, Inc. (IEEE), Piscataway, 2021-1-1, 4704-4707, 2021.

795 Li, M., He, F., Li, S., and Yang, F.: Reconstruction of the cropland cover changes in eastern china between the 10th century
796 and 13th century using historical documents, *Sci Rep*, 13552, <https://doi.org/10.1038/s41598-018-31807-6>, 2018.

797 Li, S., He, F., and Zhang, X.: Spatially explicit reconstruction of cropland cover in china from 1661 to 1996, *Reg. Envir.*
798 *Chang.*, 16, 417-428, <https://doi.org/10.1007/s10113-014-0751-4>, 2016.

799 Liu, J., Liu, B., Liu, H., and Zhang, F.: Long - term cultivation drives soil carbon, nitrogen, and bacterial community changes
800 in the black soil region of northeastern China, *Land Degrad. Dev.*, 35, 428-441, <https://doi.org/10.1002/ldr.4925>, 2024.

801 Pongratz, J., Reick, C., Raddatz, T., and Claussen, M.: A reconstruction of global agricultural areas and land cover for the last
802 millennium, *Glob. Biogeochem. Cycle*, 22, GB3018, <https://doi.org/10.1029/2007GB003153>, 2008.

803 Poschlod, P., Bakker, J. P., and Kahmen, S.: Changing land use and its impact on biodiversity, *Basic Appl. Ecol.*, 6, 93-98,
804 <https://doi.org/10.1016/j.baae.2004.12.001>, 2005.

805 Potapov, P., Turubanova, S., Hansen, M. C., Tyukavina, A., Zalles, V., Khan, A., Song, X. P., Pickens, A., Shen, Q., and Cortez,
806 J.: Global maps of cropland extent and change show accelerated cropland expansion in the twenty-first century, *Nat. Food*,
807 3, 19-28, <https://doi.org/10.1038/s43016-021-00429-z>, 2022.

808 Ramankutty, N. and Foley, J. A.: Estimating historical changes in global land cover: croplands from 1700 to 1992, *Glob.*
809 *Biogeochem. Cycle*, 13, 997-1027, <https://doi.org/10.1029/1999GB900046>, 1999.

810 Ramankutty, N., Evan, A. T., Monfreda, C., and Foley, J. A.: Farming the planet: 1. Geographic distribution of global
811 agricultural lands in the year 2000, *Glob. Biogeochem. Cycle*, 22, GB1003, <https://doi.org/10.1029/2007GB002952>, 2008.

812 Roberts, N.: How humans changed the face of Earth, *Science (American Association for the Advancement of Science)*, 365,
813 865-866, <https://doi.org/10.1126/science.aay4627>, 2019.

814 Saez-Sandino, T., Maestre, F. T., Berdugo, M., Gallardo, A., Plaza, C., Garcia-Palacios, P., Guirado, E., Zhou, G., Mueller, C.
815 W., Tedersoo, L., Crowther, T. W., and Delgado-Baquerizo, M.: Increasing numbers of global change stressors reduce soil
816 carbon worldwide, *Nat. Clim. Chang.*, <https://doi.org/10.1038/s41558-024-02019-w>, 2024.

817 Sebastiaan, L., Mathilde, J., Paul, C. S., Stephan, E., Julia, P., Eric, C., Galina, C., Axel, D., Karlheinz, E., Morgan, F., Bert,
818 G., Thomas, G., Richard, A. H., Katja, K., Alexander, K., Thomas, K., Tobias, K., Tuomas, L., Annalea, L., Denis, L.,
819 Matthew, J. M., Patrick, M., Eddy, J. M., Kim, N., Kim, N., Juliane, O., Kim, P., Casimiro, A. P., Serge, R., Corinna, R.,
820 James, R., Andrew, E. S., Andrej, V., Martin, W., and Dolman, A. J.: Land management and land-cover change have
821 impacts of similar magnitude on surface temperature, *Nat. Clim. Chang.*, 4, 389-393,
822 <https://doi.org/10.1038/nclimate2196>, 2014.

823 Shukla, J., Nobre, C., and Sellers, P.: Amazon deforestation and climate change, *Science*, 247, 1322-1325,
824 <https://doi.org/10.1126/science.247.4948.1322>, 1990.

825 Shukla, P. R., Skea, J., Calvo Buendia, E., Masson-Delmotte, V., Pörtner, H. O., Roberts, D. C., Zhai, P., Slade, R., Connors,
826 S., Van Diemen, R., Ferrat, M., Haughey, E., Luz, S., Neogi, S., Pathak, M., Petzold, J., Portugal Pereira, J., Vyas, P.,
827 Huntley, E., Kissick, K., Belkacemi, M., and Malley, J.: IPCC, 2019: Climate Change and Land: an IPCC special report
828 on climate change, desertification, land degradation, sustainable land management, food security, and greenhouse gas
829 fluxes in terrestrial ecosystems, Intergovernmental Panel on Climate Change (IPCC), 2019.

830 Thenkabail, P. S. T. P.: Global cropland-extent product at 30-m resolution (gcep30) derived from landsat satellite time-series
831 data for the year 2015 using multiple machine-learning algorithms on google earth engine cloud, U.S. Geological Survey
832 Professional Paper, 1868, 63p, <https://doi.org/https://doi.org/10.3133/pp1868>, 2021.

833 Thenkabail, P. S., Teluguntla, P. G., Xiong, J., Oliphant, A., Congalton, R. G., Ozdogan, M., Gumma, M. K., Tilton, J. C., Giri,
834 C., Milesi, C., Phalke, A., Massey, R., Yadav, K., Sankey, T., Zhong, Y., Aneece, I., and Foley, D.: Global cropland-extent
835 product at 30-m resolution (gcep30) derived from landsat satellite time-series data for the year 2015 using multiple
836 machine-learning algorithms on google earth engine cloud, U.S. Geological Survey Professional Paper, 2021, 1-63,
837 <https://doi.org/10.3133/pp1868>, 2021.

838 Wang, S., Fang, C., Chen, X., Liang, J., Liu, K., Feng, K., Hubacek, K., and Wang, J.: China's ecological footprint via biomass

839 import and consumption is increasing, *Commun. Earth Environ.*, 5, 212-244, [https://doi.org/10.1038/s43247-024-01399-](https://doi.org/10.1038/s43247-024-01399-3)
840 3, 2024.

841 Wang, Y., Yu, H., Wang, S., Li, H., and Wang, Y.: Unveiling trends and environmental impacts of global black soil crop
842 production: a comprehensive assessment, *Resources, Conservation and Recycling*, 208, 107717,
843 <https://doi.org/10.1016/j.resconrec.2024.107717>, 2024.

844 Wei, X., Ye, Y., Zhang, Q., and Fang, X.: Reconstruction of cropland change over the past 300 years in the Jing-Jin-Ji area,
845 China, *Reg. Environ. Change*, 2097-2109, 2016.

846 Wei, X., Widgren, M., Li, B., Ye, Y., Fang, X., Zhang, C., and Chen, T.: Dataset of 1 km cropland cover from 1690 to 1999 in
847 Scandinavia., *Earth Syst. Sci. Data*, 3035-3056, 2021.

848 Winkler, K., Fuchs, R., Rounsevell, M., and Herold, M.: Global land use changes are four times greater than previously
849 estimated, *Nat. Commun.*, 12, 2501, <https://doi.org/10.1038/s41467-021-22702-2>, 2021.

850 Wu, Z., Fang, X., Jia, D., and Zhao, W.: Reconstruction of cropland cover using historical literature and settlement relics in
851 farming areas of shangjing dao during the liao dynasty, china, around 1100 ad, *The Holocene*, 30, 1516-1527,
852 <https://doi.org/10.1177/0959683620941293>, 2020.

853 Wu, Z., Fang, X., and Ye, Y.: A settlement density based allocation method for historical cropland cover: a case study of jilin
854 province, china, *Land*, 11, 1374, <https://doi.org/10.3390/land11081374>, 2022.

855 Xu, M., Zhang, Z., Yue, C., Zhao, J., Zhang, P., Wang, M., Wang, J., Zhao, H., Liu, J., Tang, X., and He, J.: Contributions of
856 China's terrestrial ecosystem carbon uptakes to offsetting CO₂ emissions under different scenarios over 2001–2060, *Glob.*
857 *Planet. Change*, 238, 104485, <https://doi.org/10.1016/j.gloplacha.2024.104485>, 2024.

858 Xuan, X., Zhang, F., Deng, X., and Bai, Y.: Measurement and spatio-temporal transfer of greenhouse gas emissions from
859 agricultural sources in China: a food trade perspective, *Resources, Conservation and Recycling*, 197, 107100,
860 <https://doi.org/10.1016/j.resconrec.2023.107100>, 2023.

861 Yang, F., Dong, G., Wu, P., and He, F.: Stylized facts of past 1000-year of China's cropland changes, *Land Use Policy*, 144,
862 107258, <https://doi.org/10.1016/j.landusepol.2024.107258>, 2024.

863 Yang, J. and Huang, X.: The 30 m annual land cover dataset and its dynamics in china from 1990 to 2019, *Earth Syst. Sci.*
864 *Data*, 13, 3907-3925, <https://doi.org/10.5194/essd-13-3907-2021>, 2021.

865 Yang, Y., Zhang, S., Liu, Y., Xing, X., and De Sherbinin, A.: Analyzing historical land use changes using a historical land use
866 reconstruction model: a case study in zhenlai county, northeastern china, *Sci Rep*, 7, 41275,
867 <https://doi.org/10.1038/srep41275>, 2017.

868 Ye, X., Garber, P. A., Li, M., and Zhao, X.: Climate and anthropogenic activities threaten two langur species irrespective of
869 their range size, *Diversity & Distributions*, 30, n/a, <https://doi.org/10.1111/ddi.13841>, 2024.

870 Ye, Y. Wei, X. Li, F. and Fang, X.: Reconstruction of cropland cover changes in the Shandong Province over the past 300 years,
871 Sci. Rep., 13642, <https://doi.org/10.1038/srep13642>, 2015. Ye, Y. and Fang, X.: Expansion of cropland area and formation
872 of the eastern farming-pastoral ecotone in northern china during the twentieth century, *Reg. Envir. Chang.*, 923-934,
873 <https://doi.org/10.1007/s10113-012-0306-5>, 2012.

874 Ye, Y., Fang, X., Ren, Y., Zhang, X., and Chen, L.: Cropland cover change in northeast china during the past 300 years, *Science*
875 *China Earth Sciences*, 52, 1172-1182, <https://doi.org/10.1007/s11430-009-0118-8>, 2009.

876 Yu, Z., Jin, X., Miao, L., and Yang, X.: A historical reconstruction of cropland in china from 1900 to 2016, *Earth Syst. Sci.*
877 *Data*, 13, 3203-3218, <https://doi.org/10.5194/essd-13-3203-2021>, 2021.

878 Yu, Z. A. L. C.: Largely underestimated carbon emission from land use and land cover change in the conterminous United
879 States., *Glob. Change Biol.*, 3741-3752, 2019.

880 Yu, Z. and Lu, C.: Historical cropland expansion and abandonment in the continental U.S. During 1850 to 2016, *Glob. Ecol.*
881 *Biogeogr.*, 27, 322-333, <https://doi.org/10.1111/geb.12697>, 2018.

882 Zanaga, D. V. D. K.: Esa worldcover 10m 2020 v100, <https://doi.org/https://doi.org/10.5281/zenodo.5571936>, 2021.

883 Zhang, C., Fang, X., Ye, Y., Tang, C., Wu, Z., Zheng, X., Zhang, D., Jiang, C., Li, J., Li, Y., and Zhao, Z.: A spatially explicit
884 reconstruction of cropland cover in china around 1850 c.e. Employing new land suitability based gridded allocation
885 algorithm, *Quat. Int.*, 641, 62-73, <https://doi.org/10.1016/j.quaint.2022.06.001>, 2022.

886 Zhang, L., Jiang, L., Zhang, X., Zhang, A., and Jiang, C.: Reconstruction of cropland over heilongjiang province in the late
887 19th century, *Acta Geographica Sinica*, 69, 448-458, <https://doi.org/10.11821/dlxb201404002>, 2014.

888 Zhang, X., Zhao, T., Xu, H., Liu, W., Wang, J., Chen, X., and Liu, L.: Glc_fcs30d: the first global 30-m land-cover dynamic
889 monitoring product with a fine classification system from 1985 to 2022 using dense time-series landsat imagery and
890 continuous change-detection method, *Earth Syst. Sci. Data*, 2023, 1-32, <https://doi.org/10.5194/essd-2023-320>, 2023.

891 Zhao, Y., Wang, K., Zhao, B., and Wang, F.: Spatio-temporal process and pattern of the establishment of county-level
892 administrative divisions in China in the past 2200 years, *Acta Geographica Sinica*, 79, 890-908,
893 <https://doi.org/10.11821/dlxb202404005>, 2024.

894 East Branch Railway Administration Of Russia and South Manchuria Railways Co.: North manchuria and east branch railway,
895 Volume 1, South Manchuria Railways Co., Dalian, China, 1923 (in Japanese).

896 East Branch Railway Administration Of Russia and South Manchuria Railways Co.: North manchuria and east branch railway,
897 Volume 2, South Manchuria Railways Co., Dalian, China, 1923 (in Japanese).

898 Office Of The Governor-General Of Kwantung: Economic Statistics of Manchuria and Mongolia, Office of the Governor-
899 General of Kwantung, Dalian, China, 1918 (in Japanese).

900 Cao, S. and Ge, J.: The History of Chinese Population, Volume 4, Fudan University Press, Shanghai, China, 2005b (in Chinese).

901 Cao, S. and Ge, J.: The History of Chinese Migration, Volume 5, Fudan University Press, Shanghai, China, 2022 (in Chinese).

902 Committee Of Integrative Survey Of Natural Resources and Committee Of National Planning Of Chinese Academy Of
903 Sciences: Data Compilation of National Land Resources, Volume 1, Committee of National Planning of Chinese Academy
904 of Sciences, 1989 (in Chinese).

905 Committee Of Integrative Survey Of Natural Resources and Committee Of National Planning Of Chinese Academy Of
906 Sciences: Data Compilation of National Land Resources, Volume 3, Committee of National Planning of Chinese Academy
907 of Sciences, Beijing, China, 1990 (in Chinese).

908 Cong, P.: Garrison Reclamation in Liaodong in the Ming Dynasty, *Journal of Chinese Historical Studies*, 93-107, 1985 (in
909 Chinese).

910 Cong, P.: Agriculture in Liaoyang Province in the Yuan Dynasty, *Northern Cultural Relics*, 78-88,
911 <https://doi.org/10.16422/j.cnki.1001-0483.1993.01.019>, 1993a (in Chinese).

912 Cong, P.: Khitan, Goryeo, Semu and Mongolian in Liaoyang Province in the Yuan Dynasty, *Collected Papers of History Studies*,
913 7-14, 1993b (in Chinese).

914 Cropland Research Group: Quantitative Economic Analysis of Cropland Decline in China, Economic Science Press, Beijing,
915 China, 1992 (in Chinese).

916 Fan, X.: Research on the Mechanism of the Layout of Ming Great Wall Military Defense System, Ph.D. thesis, Tianjin
917 University, 324 pp., 2015 (in Chinese).

918 Fang, X., He, F., Wu, Z., and Zheng, J.: General characteristics of the agricultural area and fractional cropland cover changes
919 in China for the past 2000 years, *Acta Geographica Sinica*, 1732-1746, <https://doi.org/10.11821/dlxb202107012>, 2021 (in
920 Chinese). Fang, X., Ye, Y., Ge, Q., and Zheng, J.: Land Exploitation in the Northeast China during the Qing Dynasty
921 Inferred from the Development of Town System, *Scientia Geographica Sinica*, 25, 129-134,
922 <https://doi.org/10.3969/j.issn.1000-0690.2005.02.001>, 2005 (in Chinese).

923 Fang, X., Ye, Y., and Zeng, Z.: Interaction of extreme climate event—cultivation—policy management, *Science China Earth
924 Sciences*, 36, 680-688, <https://doi.org/10.3969/j.issn.1674-7240.2006.07.009>, 2006 (in Chinese).

925 Ge, J.: The History of Chinese Population, Volume 1, Fudan University Press, Shanghai, China, 2002 (in Chinese).

926 Han, M.: Historical agricultural geography of China, Peking University Press, Beijing, China, 2012 (in Chinese).

927 Han, M.: Agricultural Geography of Liao and Jin Dynasties, Social Sciences Academic Press, Beijing, China, 1999 (in Chinese).

928 Inner Mongolia Provincial Bureau Of Statistics: Agricultural and animal husbandry production statistics, Inner Mongolia
929 Provincial Bureau of Statistics, Hohhot, China, 1983 (in Chinese).

930 Jin, Q. and Mikami, T.: Research on Jurchen in Jin Dynasty, Heilongjiang People's Publishing House, Harbin, China, 1984 (in
931 Chinese).

- 932 Kong, J. and Feng, Y.: Historical Geography of Northeast China, Heilongjiang People's Publishing House, Harbin, China, 1989
933 (in Chinese).
- 934 Li, M.: Reconstruction of cropland change data for eastern Asia and its spatial-temporal characteristics analysis in the last
935 millennium, Ph.D. thesis, University of Chinese Academy of Sciences, China, 176 pp., 2019 (in Chinese).
- 936 Li, Y.: Land Resources of China, China Land Press, Beijing, China, 2000 (in Chinese).
- 937 Liu, P.: A Study of registered residence in Jin Dynasty, Study of Chinese History, 86-96, 1994a (in Chinese).
- 938 Liu, P.: A Study on the population status of Meng'an Mouke in Jin Dynasty, Ethno-National Studies, 81-89, 1994b (in Chinese).
- 939 Liu, Z., Han, G., and Liu, H.: Quan Liao Zhi (ed. in 1566), Science Press, Beijing, China, 2016 (in Chinese).
- 940 National Bureau Of Statistics: China Statistical Yearbook, China Statistics Press, Beijing, China, 2023 (in Chinese).
- 941 National Bureau Of Statistics: The Summary of Rural Social Economic Statistics on County Level in China, Chinese Statistical
942 Press, Beijing, China, 1989 (in Chinese).
- 943 Shi, F.: History Draft of Chinese Population Migration, Heilongjiang People's Publishing House, Harbin, China, 1990 (in
944 Chinese).
- 945 Shi, Z.: An Estimate of Agricultural Economic Indicators in the Qing Dynasty, Researches in Chinese Economic History, 5-
946 30, 2015 (in Chinese).
- 947 South Manchuria Railways Co.: Weights and Measures in Northeast China, South Manchuria Railways Co., Dalian, China,
948 1927 (in Japanese).
- 949 Song, L.: Dynastic History of Yuan Dynasty, Zhonghua Publishing House, Beijing, China, 1976 (in Chinese).
- 950 Tan, Q.: The Historical Atlas of China, Volume 7, SinoMaps Press, Beijing, China, 1982a (in Chinese).
- 951 Tan, Q.: The Historical Atlas of China, Volume 6, SinoMaps Press, Beijing, China, 1982b (in Chinese).
- 952 Tian, Y.: The land use and land cover change in Re-Cha-Sui area in recent 300 years, Master. thesis, Graduate School of
953 Chinese Academy of Sciences, 166 pp., 2005 (in Chinese).
- 954 Toqto'A: Dynastic History of Liao Dynasty, Zhonghua Publishing House, Beijing, China, 1974 (in Chinese).
- 955 Toqto'A: Dynastic History of Jin Dynasty, Zhonghua Publishing House, Beijing, China, 1975 (in Chinese).
- 956 Wang, Y.: Garrison Reclamation of the Ming Dynasty, Zhonghua Publishing House, Beijing, China, 2009 (in Chinese).
- 957 Wu, S. and Ge, J.: The History of Chinese Population, Volume 3, Fudan University Press, Shanghai, China, 2005a (in Chinese).
- 958 Wu, S. and Ge, J.: The History of Chinese Migration, Volume 4, Fudan University Press, Shanghai, China, 2022 (in Chinese).
- 959 Wu, Z.: Development of Gridded Allocation Method for Historical Cropland Based on Settlement Information and Its
960 Application, Ph.D. thesis, Beijing Normal University, China, 184 pp., 2021 (in Chinese).
- 961 Xiong, Z.: Summary of county governance in Northeast China, Lida Publishing House, 1933 (in Chinese).
- 962 Xu, X., Li, B., Liu, X., Li, X., and Shi, Q.: Mapping annual global land cover changes at a 30 m resolution from 2000 to 2015,

963 National Remote Sensing Bulletin, 1896-1916, <https://doi.org/10.11834/jrs.20211261>, 2021 (in Chinese).

964 Xue, L.: Research of the Governance Over the Northeast Region in the Yuan Dynasty, Social Sciences Academic Press, Beijing,
965 China, 2012 (in Chinese).

966 Xue, L.: Research on the Liaoyang Province and Governance over the Northeast China of the Yuan Dynasty, Ph.D. thesis,
967 Nankai University, 261 pp., 2006 (in Chinese).

968 Ye, Y., Fang, X., Dai, Y., Zeng, Z., and Zhang, X.: Calibration of cropland data and reconstruction of rate of reclamation in
969 Northeast China during the period of Republic of China, *Progress in Natural Science*, 16, 1419-1427, 2006 (in Chinese).

970 Zeng, Z., Fang, X., and Ye, Y.: The Process of Land Cultivation Based on Settlement Names in Jilin Province in the Past 300
971 Years, *Acta Geographica Sinica*, 985-993, 2011 (in Chinese).

972 Zhan, J.: Heilongjiang History of Land Reclamation in border Areas, Volume 1, Social Sciences Academic Press, Beijing,
973 China, 2017 (in Chinese).

974 Zhang, L., Fang, X., Ren, G., and Suo, X.: Environmental Changes in the North China Farming Grazing Transitional Zone,
975 *Earth Science Frontiers*, 127-136, <https://doi.org/10.3321/j.issn:1005-2321.1997.01.015>, 1997 (in Chinese).

976 Zhang, T.: Dynastic History of Ming Dynasty, Zhonghua Publishing House, Beijing, China, 1974 (in Chinese).

977 Zhang, Y.: Re-estimation on China's population and cropland in modern times, *Researches in Chinese Economic History*, 20-
978 30, 1991 (in Chinese).

979 Zhou, S.: Study of Jurchen in Liaoyang Province in the Yuan Dynasty, Shanghai Jiaotong University Press, Shanghai, China,
980 2021 (in Chinese).

981 Zhou, R.: A General Inspection and Re-appraise on Area Under Cultivation in the Early Period of the Qing, *Journal of Chinese
982 Social and Economic History*, 39-49, <https://doi.org/10.3969/j.issn.1000-422X.2001.03.004>, 2001 (in Chinese).